Rapid optical variability of TeV blazars

Gopal-Krishna[1][*], Arti Goyal[1,2], S. Joshi[2], Chrisphin Karthick[2], R. Sagar[2],
Paul J. Wiita[3], G. C. Anupama[4], D. K. Sahu[4]

[1] *National Centre for Radio Astrophysics/TIFR, Pune University Campus, Pune 411 007, India*

[2] *Aryabhatta Research Institute of Observational Sciences (ARIES), Manora Peak, Naini Tal 263 129, India*

[3] *Department of Physics, The College of New Jersey, P.O. Box 7718, Ewing, NJ 08628, USA*

[4] *Indian Institute of Astrophysics (IIA), Bangalore 560 034, India*

Released 2002 Xxxxx XX

ABSTRACT

In this first systematic attempt to characterise the intranight optical variability (INOV) of TeV detected blazars, we have monitored a well defined set of 9 TeV blazars on total 26 nights during 2004-2010. In this R (or V)-band monitoring programme only one blazar was monitored per night and the minimum duration was close to 4 hours, the average being 5.3 hours per night. Using the CCD for strictly simultaneous photometry of the blazar and nearby reference stars (N-star photometry), an INOV detection threshold of $\sim$ 1–2 per cent was achieved in the densely sampled differential light curves derived from our data. We have further expanded the sample by including another 13 TeV blazars, taking advantage of the availability in the literature of INOV data, including those published earlier in our programme. The selection criteria for this set of 13 blazars conform to the basic criteria we had adopted for the first set of 9 blazars we have monitored presently. This enlarged, well defined representative sample of 22 TeV blazars, monitored on a total of 116 nights (including 55 nights newly reported here), has enabled us to arrive at the first estimate of the INOV duty cycle (DC) of TeV detected blazars. Applying the conservative, but commonly employed, C-test, the INOV DC is found to be 59 per cent, which decreases to 47 per cent if only INOV fractional amplitudes (ψ) above 3 per cent are considered. These observations also permit, for the first time, a comparison of the INOV characteristics of the two

major subclasses of TeV detected BL Lacs, namely LBLs and HBLs, for which we find the INOV duty cycles to be ~ 63 per cent and ~ 38 per cent, respectively. This demonstrates that the previously recognized INOV differential between LBLs and HBLs persists even when only their TeV detected subsets are considered. Despite dense sampling, the intranight light curves of the 22 TeV blazars have not revealed even a single feature on time scale substantially shorter than 1 hour, even though the inner jets of TeV blazars are believed to have exceptionally large bulk Lorentz factors (and correspondingly stronger time compression). An intriguing feature, clearly detected in the light curve of the HBL J1555+1111, is a 4 per cent 'dip' on a 1 hour timescale. This unique feature could have arisen from absorption in a dusty gas cloud, occulting a superluminally moving optical knot in the parsec scale jet of this relatively luminous BL Lacs object.

Key words:

galaxies: active — galaxies: jets — BL Lacertae objects: general — galaxies: photometry

1 INTRODUCTION

Intensity variations have long been recognized as a defining characteristic of active galactic nuclei (AGN). Variability is a powerful tool for probing AGN geometry and physical properties such as the black hole mass, and the sizes and bulk motions of the outflows in their innermost regions that are well beyond the current imaging capabilities of telescopes in any part of the electromagnetic spectrum (e.g., Wagner & Witzel 1995; Urry & Padovani 1995; Xie et al. 2001). The variations can be particularly violent for those AGNs whose flux is dominated by relativistic jets of nonthermal radiation broadly pointing in our direction (e.g., Begelman, Blandford & Rees 1984). Intensities of such AGNs, called 'blazars', are known to vary across the entire electromagnetic spectrum and time scales from minutes to years have been observed. For instance, in the soft X-ray band, several TeV emitting blazars have been found to vary on a characteristic time scale of $\sim$1 day, with the flares having sub-structures on shorter time scales of $\sim 10^4$s (e.g., Tanihata et al. 2001; Kataoka et al. 2001). In the optical regime, there have been many detections of intra-night optical variability (INOV), or optical microvariability, following the pioneering work of Carini, Miller & Goodrich (1990)

* E-mail: krishna@ncra.tifr.res.in

who first used CCD detectors as multi-object photometers for this purpose. The shortest time scale found for essentially all INOV events is around 1 hour, with an amplitude of a few percent (e.g., Xie et al. 2001; Romero et al. 2002; Stalin et al. 2004a). Such rapid continuum variability of blazars is usually explained by invoking relativistic jets (e.g., Marscher 1996; Schlickeiser 1996; Wiita 2006).

A study of 23 AGN of the quasar/Seyfert1 type (i.e., non-blazar) yielded a 1σ upper limit of 0.03 mag for variability on hour-like timescales (Webb & Malkan 2000). The literature does contain reports of a few INOV detections on time scales much shorter than 1 hour. Examples include the papers by Kidger & deDiego (1990), Sagar, Gopal-Krishna & Wiita (1996), Xie et al. (2001), and Dai et al. (2001); however, see Romero et al. (2002) for a convincing critique of the latter two claims. To our knowledge such assertions are lacking in the literature over the past 5 years or so, aside from a very recent paper presenting evidence for a quasi-periodic oscillation of $\simeq$ 15 min spanning most of a night of optical monitoring of the TeV blazar S5 0716+714 (Rani et al. 2010), which is also a member of our present sample. Very recently, Impiombato et al. (2011) have reported a single event of duration $\sim$25 minutes in J-band while searching for long and short term optical and infrared variability for blazar PKS0537$-$441 in the data spanning for $\sim$6 years (2004-2009). There is thus a need for renewed efforts capable of making robust detections of events of ultra-rapid INOV events on sub-hour time scales.

Since $\gamma-$ray emission is known to be correlated with relatively large bulk Doppler factors of the radiating plasma in the blazar jets for both the GeV band probed by EGRET (e.g., Kellermann et al. 2004; Lister & Homan 2005) and the higher energies probed by Fermi/LAT (Kovalev et al. 2009; Savolainen et al. 2010), TeV blazars appear to be particularly promising candidates for detecting the most rapid INOV. In TeV blazars, the relativistic plasma of the inner jets almost certainly must move with a bulk Lorentz factor $\Gamma \geqslant 45$–50 in order to escape absorption of the TeV photons due to the pair production process in the radiation field present near the origin (e.g., Krawczynski, Coppi & Aharonian 2002; Begelman, Fabian & Rees 2008; for large Lorentz factors in blazar jets, also see Kundt & Gopal-Krishna 1980, 2004). According to one model, such ultra-fast moving emission features may arise in situ within the jet, e.g., from reconnection events in a Poynting flux dominated jet (Giannios, Uzdensky & Begelman 2009). Thus, it seems likely that in TeV blazars the bulk Lorentz factors of the optically radiating inner segments of the jets are also comparatively larger than those occuring in other blazars. Here we note that the marked paucity of apparent

superluminal motion in the jets of TeV blazars, highlighted by Piner & Edwards (2004), can be reconciled with the above requirement of extreme bulk Lorentz factors in a number of ways, e.g., by taking into account a modest opening angle for the jet (Gopal-Krishna, Dhurde & Wiita 2004; Gopal-Krishna, Wiita & Dhurde 2006; Gopal-Krishna et al. 2007; Petrucci, Boutelier & Henri 2010), or by postulating a spine-sheath geometry for the sub-parsec scale jets (e.g., Attridge, Roberts & Wardle 1999; Ghisellini, Haardt & Matt 2004) or, alternatively, if the bulk of the $\gamma-$rays come from an ultra-relativistically approaching volume element in the jet (e.g., Giannios et al. 2009; also, Gopal-Krishna, Singal & Krishnamohan 1984).

In Sect. 2 we describe the selection of our sample of TeV blazars for intranight optical monitoring. Our observations are described in Sect. 3 and the results summarized in Sect. 4, followed by a discussion in Sect. 5.

2   SAMPLE SELECTION FOR TEV BLAZARS

Our sample of TeV blazars consists of two sets. Set 1 is derived from the list of TeV detected extragalactic AGN, published by Weekes (2008; Table 2 of his paper). Application of the criteria, $z > 0.1$, $\delta > -10°$ and $m_B \leqslant 18$ to that list leaves us with 9 TeV blazars. The redshift limit is designed to exclude the nearest blazars so that the optical image should have a point-like appearence. This is to ensure that the host galaxy makes a negligible contribution to the image, a pre-requisite for high precision photometry. The declination and the apparent magnitude limits are meant to ensure a sufficiently dense sampling and reasonably long duration ($\gtrsim 4$ hours) for the continuum light curves obtained with the $1-2$ metre class telescopes employed in this programme. The 9 TeV blazars constituting Set 1 are: TeV1219+283, TeV1429+427, TeV0809+524, TeV1218+304, TeV1011+496, TeV0716+714, TeV1553+11, TeV0219+425 and TeV1256$-$058, listed in increasing order of distance from us. The intra-night and long-term optical lightcurves of these 9 blazars are derived in this study and presented here.

Our Set 2 of TeV blazars was derived from Table 1 of Abdo et al. (2010), consisting of 709 TeV detected AGNs, which is based on 11 months of monitoring with Fermi LAT. This set consists of 13 blazars, including 10 high polarization core-dominated quasars (HPCDQs) and 3 BL Lac objects. The HPCDQs were selected employing the following criteria: all CDQs labeled "HP" ($P_{op} > 3$ per cent) in the compendium of Véron & Véron (2006) were

subjected to the aforementioned selection criteria, namely, $z > 0.1$, $\delta > -10°$ and $m_B \leqslant 18$. To ensure the availability of INOV data additional selection filters used are:

(a) We selected all the 7 HPCDQs from J. Noble's PhD thesis (Noble 1995, Table 3.1). These are J0239+1637, J1159+2914, J1256−0547, J1310+3220, J1643+3953, J2225−0457, J2253+1608. Of these J1256−0547 (3C 279) is already a member of Set 1 and J1643+3953 (3C 345) is undetected by Fermi LAT. This gave us the first 5 TeV blazars for Set 2.

(b) Another 3 HPCDQs were taken from the polarimetric survey of Wills et al. (1992), limiting ourselves to the right ascension range 03^h – 15^h and declination range $-10°$ to $+40°$. Note that although these criteria yielded 5 HPCDQs (J0423−0120, J0739+0136, J1058+0133, J1159+2914 and J1256−0547), the last two of these are already a part of the Noble (1995) sample (a). This left us with 3 additional blazars.

(c) One HPCDQ, J1218−0119, was taken from the first phase of our INOV program (Sagar et al. 2004, Stalin et al. 2005). INOV data have been taken from those papers for this source as well as for another two HPCDQs (J0239+1637 and J1310+3220) that are in the part (a) of Set 2 derived from Noble (1995). Note that these were the only 3 HPCDQs monitored in the first phase of our INOV program.

(d) Lastly, one HPCDQ was added from the sample of Romero, Cellone & Combi (1999). They have reported V-band intranight monitoring of a sample of southern AGN that contains 4 HPCDQs, according to the Véron & Véron (2006) classification. These are J0538−4405, J1147−3812, J1246−2547, and J1512−0906. Only the last of these HPCDQs was included in our sample; because we could ensure a minimum 3 nights' monitoring data; the others are situated far to the south.

(e) We have also included the 3 BL Lacs PKS 0735+178, OJ 287 and B2 1215+30 for which intra-night monitoring data of duration $\gtrsim 4$ hours are available in the literature. This completes our Set 2 that contains 13 TeV detected blazars.

Salient properties of the two blazar sets are listed in Table 1. All these sources have flat radio spectra ($\alpha_r > -0.5$, where $S(\nu) \propto \nu^{\alpha_r}$) as well as high optical linear polarization, with P_{op} falling in the range 3.5 to 44 per cent, except for J1428+4240 (which has a slightly steep integrated radio spectrum with $\alpha_r \simeq -0.58$, and a comparatively low optical polarization, $P_{op} = 2.5\%$). The values of radio core luminosity (P_c), extended radio luminosity (P_{ext}), and the radio core-dominance parameter (f_c; ratio of core to extended radio luminosities) at 5 GHz, were determined using the available Very Long Baseline Interferometry (VLBI) measurements at milli-arcsecond resolution and the integrated NRAO VLA Sky Survey

(NVSS) flux values at 1.4 GHz, taking a radio spectral index of zero for the core ($\alpha_c = 0$) and $\alpha_{ext} = -0.5$ for the extended emission. The concordance cosmological model was assumed, with a Hubble constant $H_0 = 70$ km sec^{-1} Mpc^{-1}, $\Omega_m = 0.3$ and $\Omega_\Lambda = 0.7$ (Spergel et al. 2007). Values of the radio loudness parameter (R^*) were determined following Stocke et al. (1992). The absolute magnitudes, M_B, were calculated taking the total galactic extinction from Schlegel, Finkbeiner & Davis (1998) and assuming an optical spectral index α_{op} of -0.7.

3   OBSERVATIONS

3.1   Instruments used

The observations were mainly carried out using the 104-cm Sampurnanand telescope (ST) located at the Aryabhatta Research Institute of observational sciencES (ARIES), in Naini Tal, India. It has Ritchey-Chrétien (RC) optics with a f/13 beam (Sagar 1999). The detector was a cryogenically cooled 2048×2048 chip mounted at the Cassegrain focus. This chip has a readout noise of 5.3 e$^-$/pixel and a gain of 10 e$^-$/Analog to Digital Unit (ADU) in the usually employed slow readout mode. Each pixel has a dimension of 24 μm^2 which corresponds to 0.37 arcsec^2 on the sky, covering a total field of $13' \times 13'$. Observations were carried out in 2×2 binned mode to improve the S/N ratio. All the observations with the ST were carried out using an R filter for which the CCD sensitivity is maximum. The seeing ranged mostly between $\sim 1''.5$ and $\sim 3''$, as determined using 3 moderately bright stars within the CCD frame. For each night, the plot of seeing is provided in Figure 1 in the corresponding bottom panel.

The other telescope used for our monitoring of TeV blazars is the 201-cm Himalayan Chandra Telescope (HCT) of the Indian Astronomical Observatory (IAO) located at Hanle, India, which is also of the RC design with a f/9 beam at the Cassegrain focus[1]. The detector was a cryogenically cooled 2048×4096 chip, of which the central 2048×2048 pixels were used. As the pixel size is 15 μm^2 the image scale of 0.29 arcsec/pixel covers an area of $10' \times 10'$ on the sky. The readout noise of the CCD is 4.87 e$^-$/pixel and the gain is 1.22 e$^-$/ADU. This CCD was used in an unbinned mode. The seeing ranged mostly between $\sim 1''$ to $\sim 3''$.

Lastly, one night of blazar monitoring data were obtained using the 200-cm IUCAA

---

[1] http://www.iiap.res.in/~iao

Girawali Observatory (IGO) telescope located near Pune, India. It has an RC design with a f/10 beam at the Cassegrain focus[2]. The detector was a cryogenically cooled 2110×2048 chip mounted at the Cassegrain focus. The pixel size is 15 μm^2 so that the image scale of 0.27 arcsec/pixel covers an area of $10' \times 10'$ on the sky. The readout noise of this CCD is 4.0 e$^-$/pixel and the gain is 1.5 e$^-$/ADU. The CCD was used in an unbinned mode. The seeing ranged between $\sim 1''.0$ and $\sim 1''.5$ on that particular night.

The observations were made using R or V filters. The exposure times were typically 10 to 12 minutes for the ARIES and IGO observations and ranged between 3 to 6 minutes for the observations from IAO (depending on the brightness of the source, the lunar phase and the sky transparency for the night). The field positioning was adjusted so as to always have within the CCD frame 2–3 comparison stars within about a magnitude of the blazar, in order to minimize the possibility of getting spurious variability detection (e.g., Cellone, Romero & Araudo 2007). For all three telescopes, bias frames were taken intermittently and twilight sky flats were obtained on each night. Each blazar in Set 1 was monitored for a minimum of 3 nights. Likewise, for the blazars in Set 2, this requirement of minimum 3 nights is met, except for the case of J2253+1608 (3C 454.3) for which only 2 nights' of monitoring data are available.

3.2   Data reduction

The preprocessing of the images (bias subtraction, flat-fielding and cosmic-ray removal) was done by applying the standard procedures in IRAF[3] and MIDAS[4] softwares. The instrumental magnitudes of the blazar and the comparison stars in the image frames were determined by aperture photometry using DAOPHOT II[5] (Stetson 1987). The magnitude of the blazar was measured relative to the steady comparison stars present on the same CCD frame (Table 2). In this manner, Differential Light Curves (DLCs) of each blazar were produced relative to 3 comparison stars (Fig. 1). For each night, the selection of optimum aperture size for the photometry was done by examining the observed dispersions in the star-star DLCs for different aperture radii starting from the median seeing (FWHM) value on that night to 4

---

[2] http://www.iucaa.ernet.in/%7Eitp/igoweb/igo_ tele_ and_ inst.htm
[3] Image Reduction and Analysis Facility (http://iraf.noao.edu/)
[4] Munich Image and Data Analysis System (http://www.eso.org/sci/data-processing/software/esomidas//)
[5] Dominion Astrophysical Observatory Photometry software

times that value. We selected the aperture that showed minimum scatter for the steadiest DLC found for the various pairs of the comparison stars (e.g., Stalin et al. 2004a).

4   RESULTS

4.1   Variability criteria and duty cycles

The INOV DLCs are shown in Figure 1 for all the 9 blazars of Set 1. From Set 2 we present here the DLCs for just J0854+2006 (OJ 287) since it was also monitored in the present work (Fig. 1). The DLCs for another few members of the Set 2, which too were monitored in the present work, can be found in Goyal et al. (2011) as they form part of the samples discussed in that paper. Figure 2 displays the long-term optical variability (LTOV) DLCs for sources that could be observed in the same colour filter on a minimum of 3 nights. Table 3 summarizes the observations and the derived results for our entire sample of 22 TeV blazars, 9 of which were monitored in the present study (Set 1), while for the remainder (Set 2) the INOV data were largely taken from the literature (Sect. 2; Table 3). The 6th, 7th and 8th columns give, respectively, the monitoring duration on the respective night, the number of data points (N_{points}) in the DLC, and the rms of the steadiest star–star DLC obtained using two of the comparison stars.

The next columns in Table 3 contain the measures of the source variability (INOV) on each night. The fractional amplitude of INOV, ψ, is given in Col. (9), while C_{eff}, a widely used indicator of variability status, is in Col. (10). The classification 'variable' (V) or 'non-variable' (N) as decided using the C-test, basically defined following the criteria of Jang & Miller (1997), is in Col. (11).

C_{eff} for a night is derived by combining the C-values estimated for individual DLCs of the blazar on that night. For a given DLC, C is defined as the ratio of its standard deviation, σ_T and $\eta\sigma_{err}$, where σ_{err} is the average of the rms errors of its individual data points. As the photometric errors given by the DAOPHOT/IRAF package is known to be underestimated, a compasatory factor η is determined that would make the rms of the DLC consistent with the rms of its individual data points (see Edelson et al. 2002, also, Stalin et al. 2004a). In this way, the computed value of η is found to be ∼1.5 (Stalin et al. 2004a, 2004b, 2005; Gopal-Krishna et al. 2003; Sagar et al. 2004). However, our analysis for the present dataset yields $\eta = 1.3$ and so we have adopted this value here. We computed C_{eff} from the C values (as defined above) derived for the individual DLCs of a given blazar

relative to 3 different comparison stars which were monitored simultaneously with the blazar on the same CCD chip. This gave us 3 values of C for a given blazar. These values were converted into probabilities and multiplied to obtain C_{eff} for the blazar (Sagar et al. 2004 for details) . This has the advantage of using the available multiple DLCs of an AGN, relative to different comparison stars. The AGN is termed 'V' for $C_{\mathrm{eff}} > 2.576$, corresponding to a nominal confidence level above 0.99. The 'probable 'variable' (PV) classification applies when, $1.950 < C_{\mathrm{eff}} < 2.576$, corresponding to a nominal confidence level between 0.95 to 0.99.

It has been recently argued by de Diego (2010), however, that C is not a proper statistic as it is based on ratios of standard deviations and not on ratios of variances; only the latter are distributed in such a way that χ^2 tests can be used to assign proper confidence levels. He shows that the standard F-statistic, where

$$F = \frac{\sigma^2(blazar - star_i)}{\sigma^2(star_i - star_j)}, \tag{1}$$

is a more appropriate choice for characterizing AGN light curves. It also has the advantage that the somewhat uncertain parameter, η, cancels out. Col. 12 gives the F-value for each night along with the number of degrees of freedom shown in parentheses. Since we can compute the F-statistic only for our data, for the bulk of blazars in Set 2 (not observed by us) only the C-values are available. In computing the F-values we examined the various star–star light curves to decide if any of the comparison stars might have even slightly varied on that night. We considered the steadiest two of the three comparison stars and selected the one closer to the blazar in apparent magnitude. The two DLCs (namely, blazar−star and star−star) involving the selected comparison star were then used in the F-test (Eq. 1). For a fair comparison to the C-test, we take for the F-test a significance of > 0.99 to correspond to a definitely variable source (V) and a significance between 0.95 and 0.99 to correspond to the PV classification. These indicators of variability status as computed using F-test are tabulated in the 13th column. The last column gives the reference(s) for the INOV data used here.

The peak-to-peak INOV amplitude is calculated using the definition (Romero et al., 1999)

$$\psi = \sqrt{(D_{max} - D_{min})^2 - 2\sigma^2} \tag{2}$$

with $D_{max} =$ maximum in the AGN's differential light curve, $D_{min} =$ minimum in the AGN's differential light curve, and $\sigma^2 = \eta^2 \langle \sigma^2_{err} \rangle$.

The INOV duty cycle (DC) for our entire sample of 22 TeV blazars (Table 3) was then computed following the definition of Romero et al. (1999) (see also, Stalin et al. 2004a):

$$DC = 100\frac{\sum_{i=1}^{n} N_i(1/\Delta t_i)}{\sum_{i=1}^{n}(1/\Delta t_i)}\text{percent} \qquad (3)$$

where $\Delta t_i = \Delta t_{i,obs}(1+z)^{-1}$ is the duration of the blazar monitoring session on the ith night, corrected for the blazar's cosmological redshift, z. Note that since the monitoring durations for any given source on different nights were not equal, the computation of DC has been weighted by the actual monitoring duration Δt_i on the ith night. The parameter N_i was set equal to 1 if INOV was detected; otherwise $N_i = 0$.

We realize that 2 of our 9 blazars in Set 1 lie at rather small redshifts (Table 1; J1221+2813 at $z = 0.102$ and J1428+4240 at $z = 0.129$), raising the possibility of a significant contribution from the host galaxy to the flux falling within the circular photometry aperture centered at the blazar. As stressed by, e.g., Cellone, Romero & Combi (2000), the host's varying contribution to the flux within the aperture changes as the seeing varies and thus the atmospheric seeing changes can yield spurious INOV detection. The paper also presents simulated DLCs for AGN, relative to a suitable comparison star, for cases where the emission from the AGN host galaxy (elliptical or spiral) is comparable to that from the AGN itself and the atmospheric seeing undergoes a large intranight variation. For a wide range in the host galaxy size, they find that even if the host's flux is comparable to that of the AGN (an extreme situation from the perspective of the present sample), the DLCs show a negligible variation ($\psi < 1\%$) as long as the aperture radius exceeds $\sim 3'' - 4''$ and the seeing remains within this limit (as also applicable to the present study). Therefore, since our choice of aperture size always meets this condition, we do not expect any of our DLCs classified as 'V' to be spurious, i.e., being an artefact of variable atmospheric seeing during the night.

Note also that in a very small number of cases the INOV results taken from the literature were for the V band; however, for the present purpose we do not distinguish them from our data which were essentially always taken in the R band.

Based on the C-test the computed INOV DC for our sample of 22 TeV blazars is found to be ~ 59 per cent (116 nights; Table 3), which increases to ~ 64 per cent if five 'PV' cases of 'probable' INOV are also included. However, for the nights showing larger INOV amplitudes, $\psi > 0.03$, the INOV DC is ~ 47 per cent. Since the redshift the blazar J1555+1111 is known to be controversial, with values ranging from 0.25 to 0.50 (see, Treves, Falomo & Uslenghi,

2007 and MAGIC collaboration: Albert et al. 2008) we have computed the DC vlaues for our entire sample of blazars (116 nights), taking the lower and upper z values for J1555+1111. The computed values are $DC = 58.6\%$ and $DC = 58.9\%$, respectively. Thus, the uncertainty in z of J1555+1111 does not significantly affect the estimated DC for the sample (i.e., DC $\sim$59%). Using the F-test, the corresponding DC values for the 9 blazars monitored presently, is ~ 72 per cent (~ 76 per cent, if the two 'PV' cases are included) but only ~ 33 per cent for the cases having $\psi > 0.03$ (55 nights; Table 3).

4.2 Notes on the optical lightcurves of the TeV blazars

4.2.1 Set 1

The basic parameters for all these 9 blazars monitored by us have been taken from the compilations by Abdo et al. (2010a) and Weekes (2008) and their INOV and LTOV lightcurves determined in the present work are shown in Fig. 1 & Fig. 2, respectively. As seen from Table 1, the Set 1 of TeV blazars consists of five HBLs, two IBLs, one LBL and one FSRQ.

- J0222+4302 (3C 66A; $z = 0.444$)

This blazar (Bramel et al. 2005) has been classified as an intermediate-peaked BL Lac object (IBL) whose nonthermal emission peaks in the range $10^{15} - 10^{16}$ Hz (Perri et al. 2003). During 1998–2000 it was monitored in our programme on 7 nights, for durations ranging between 5 and 10 hours per night. INOV was detected on 6 of the nights (Sagar et al. 2004). The only sub-hour feature seen in those DLCs is a 1.5 per cent 'glitch' detected on the night of 13 Nov. 1999 at 19.6 U.T. In Table 3 we have combined those published data with the two DLCs obtained in the present work. Of these, the DLC on 28 Sept. 2009 showed confirmed INOV using both $C_{\rm eff}$ and F statistics. Also, a clear event of *internight* variability was observed when the source faded by $\sim$0.04 mag between 27 and 28 Sept. 2009 (Fig. 1).

- J0721+7120 (S5 0716+714; $z = 0.31$)

This blazar with a 'LBL' classification is the archetypal intra-day variable (e.g., Wagner et al. 1996) with a history of frequent high-amplitude flux variations (e.g., Gupta et al. 2008 and references therein). From their R-band light curves Wagner et al. (1996) had reported a significant "flickering" on time scale as short as ≈ 15 minutes. Recently, its high temporal resolution study revealed quasi-periodic oscillations of about 15 minutes at $> 3\sigma$ significance (Rani et al. 2010). The presence of such short time scales in an optical light curve can provide important clues to relativistic beaming at these wavelengths (e.g., Fabian

& Rees 1979; Guilbert, Fabian & Rees 1983). During February and March 1994 this blazar was the target of a 4-week long INOV monitoring campaign (BVRI) under our programme, using two Indian telescopes: the 1-m ST and the 2-m Vainu Bappu Telescope (Sagar et al. 1999). Ghisellini et al. (1997) have reported a multi-colour optical monitoring campaign around that time, revealing a moderately active state of this blazar. In the Indian campaign, a monitoring duration of 2–3 hours was typically achieved on each night. No evidence was found for INOV on time scale shorter than 1 hr, but 3 prominent events on ~ 3 hour time scales were detected. Also, *internight* variability with $\psi \sim 5 - 20$ per cent was frequently detected during the 4-week long Indian campaign. Results from other recent monitoring campaigns on this source performed at different sites should be available soon (J. Webb; A. Gupta, private communications).

The present one night's monitoring of this blazar detected a clear flare lasting ≈ 1 hour (Fig. 1; Table 3). However, since the 1.5 hour duration of our monitoring is much less than our selection criterion of $\gtrsim 4$ hour, we have not included this observation in the computation of DC for this blazar (Table 3). Note that neither of the aforementioned published observational campaigns revealed INOV time scale $\tau < 1$ hour, even for this highly variable blazar, except for results reported by Wagner et al. (1996) and some recent observations reported by Rani et al. (2010).

- J0809+5218 (1ES 0806+524; $z = 0.138$)

To our knowledge, the present work is the first intranight optical monitoring of this HBL (4 nights, Table 3). A highly unusual aspect of this source, as revealed by the 5 GHz VLBI observations, is a two-sided jet structure on parsec scale straddling the core (Chen et al. 2006), which itself has a brightness temperature of $\sim 10^{10}$ K, markedly lower than the inverse-Compton limit (Kellermann & Paulini-Toth 1969). These unusual characteristics are, however, consistent with the absence of strong relativistic boosting in this HBL, as also reflected by its quite stable GeV flux (Chen et al. 2006). On none of the 4 nights did we detect INOV in this blazar (Table 3), although on longer term (~ 10 month timescale), a clear fading by ~ 0.45 mag was detected. Thereafter, a distinct brightening by ~ 0.04 mag occured between the observations taken 4 days apart (Fig. 3).

- J1015+4926 (1ES 1011+496; $z = 0.212$)

Out of the 3 nights observed by us this HBL showed a clear variability on one night, as confirmed by both C_{eff} and F-statistics (Table 3; 7 Mar. 2010). On the night of 19 Feb 2010 it was found to be a probable variable using C_{eff} but classified as "V" on application

of F-statistics. On a longer time scale, a steady fading by $\sim$0.11 mag was seen over the 1−month span covered by our monitoring (Fig. 3).

- J1221+3010 (1ES 1218+304; $z = 0.182$)

Out of 3 nights observed by us this blazar showed a hint of variablity on one night on applying the F-statistics, but remained non-variable on all the three nights, according to the C_{eff} criterion (Table 3). However, on a longer term, we detected a clear fading by $\sim$0.1 mag between the first two epochs, which were separated by 10 days. This was followed by a phase of 0.4 mag brightening over $\sim$ 2 months, when it was last monitored by us (Fig. 3).

- J1221+2813 (W Comae/ON231, $z = 0.102$)

This is the nearest source in our sample and also the first intermediate type BL Lac (IBL) to be detected at TeV energies. Gupta et al. (2008) have reported R-band monitoring of this blazar on 11 Jan. 2007 for 3.24 hours, but no INOV was detected. We monitored this blazar on 4 epochs. It showed a confirmed variablity on 3 epochs using C_{eff} and on all 4 epochs when the F-test was applied (Table 3). In addition, a clear event of *internight* variation was seen when the source faded by $\sim$0.1mag between 19 and 20 Mar 2004.

- J1256−0547 (3C 279, $z = 0.536$)

This FSRQ of the OVV type was the first blazar to be detected as an EGRET/γ-ray source (Hartman et al. 1992) and the first FSRQ to be detected at very high energies (VHE, i.e. > 100 GeV) (MAGIC collaboration: Albert et al. 2008). This source is also particularly interesting, because with a redshift of 0.538, it is the most distant VHE blazar yet found (Abdo et al. 2009); a strong absorption of its VHE emission due to extragalactic background light (EBL) is expected, yet not seen (e.g., Costamante et al. 2009). Gupta et al. (2008) have reported R band intra-night monitoring with the 1-m Yunnan observatory telescope on two nights in early 2007 (for durations of 4 hour and 2.3 hours), but INOV was not detected. A negative result was also reported by Romero et al. (2002) from their V-band intranight monitoring lasting 3.8 hours on 06 Aug. 1999.

Application of either of the two statistics shows it to be a confirmed variable on all the 3 nights it was monitored by us, attaining peak-to-peak INOV amplitudes of 4, 10 and 22 per cent, respectively (Table 3). Further, the blazar brightened by $\sim$0.9 mag between the first two epochs of monitoring that were separated by about 2 months, and was about 2.0 mag fainter when last observed a little more than 3 years later (Fig. 3).

- J1428+4240 (H1426+428, $z = 0.129$)

This weak TeV source has its synchrotron emission peak at the highest frequency known for any blazar; hence termed as "extreme" HBL (Aharonian et al. 2002; also, Costamante et al. 2001). Its radio structure consists of a core surrounded by a faint halo (Giroletti et al. 2004). The light curves presented here are its first intranight optical monitoring observations. The C_{eff} values indicated it was non-variable on all 3 nights we monitored it; however, on application of the F-test it was found to be variable on 1 of the 3 nights (Table 3).

- J1555+1111 (PG 1553+113, $z = 0.360$)

This most distant HBL with a firm TeV detection (Abdo et al. 2009) is known to show a highly time dependent variability behaviour at different frequencies. Its radio structure is marked by an extremely large bend (by $\sim 110°$) of the parsec-scale jet towards the outer lobe (Rector, Gabuzda & Stocke 2003). It showed INOV on one of the two nights it was monitored during mid-1999 as part of our INOV programme (Stalin et al. 2005). Those data have been included in our computation of the INOV duty cycle (Table 3). In our monitoring, confirmed variability was detected on all 3 nights both using C_{eff} and F statistics. In the longer term, a clear brightening by ~ 0.25 mag was observed between the first two epochs of our monitoring, which were separated by almost a year. A clear case of *internight* variability also occured when the source brightened by another ~ 0.04 mag between 15 and 16 May 2010 (Fig. 3).

4.2.2 **Set 2**

Set 2 consists of 1 HBL, 3 LBLs, 8 FSRQs and 1 BL Lac object of unspecified HBL/LBL classification. Their INOV and LTOV data are available in the literature cited in Table 3. Only for OJ 287 do we present here new monitoring data taken by us on 2 nights (Table 3; Fig. 1).

- J0238+1637 (AO 0235+164; $z = 0.940$)

This LBL had been monitored by Noble (1995) on 5 nights and later on 3 nights in the first part of our programme (Sagar et al. 2004). On all these 8 nights it was found to be a confirmed variable, with ψ ranging between 5–20 per cent (Table 3). Romero et al. (2002) monitored it on another 6 nights and found ψ to range between 7–44 per cent. In addition, Goyal et al. (2011) have monitored this blazar on one night and it showed a gradual decline by ~ 7 per cent during the first 6 hours on that night. Thus, the INOV duty cycle of this BL Lac is essentially 100 per cent!

- J0423−0120 (PKS 0420−01; $z = 0.915$)

This blazar has been newly monitored by us on 3 nights, covering a 7 years time span (Goyal et al. 2011) It showed a confirmed variability on 19 Nov. 2003, with an INOV amplitude of $\psi \sim 2$ per cent and was a 'probable variable' on 25 Oct. 2009 (C-test). The F-test shows it to be a confirmed variable on all the 3 nights. As for LTOV, it faded by $\sim$1.9-mag between the first 2 epochs of monitoring roughly a year apart and then brightened by $\sim$0.8-mag when we last monitored it on 25 Oct. 2009.

- J0738+1742 (PKS 0735+178; $z > 0.424$)

This blazar is a rather unique case of relative intra-night quiescence that has persisted over the past two decades (Goyal et al. 2009; Britzen et al. 2010), although mild INOV (ψ <3 per cent) was detected on 5 out of the total 17 nights. On month-like timescale it has exhibited $\sim$0.5 mag variations (Sagar et al. 2004; Ciprini et al. 2007; Goyal et al. 2009).

- J0739+0137 (PKS 0736+01; $z = 0.191$)

Not only did this highly polarized CDQ remain a confirmed variable (by both C & F statistics) on 2 of the 3 nights of our monitoring (Goyal et al. 2011), it also showed a clear *internight* variability, fading by ~ 4 per cent between 5 and 6 Dec. 2005.

- J0854+2006 (OJ 287; $z = 0.306$)

This LBL was monitored by Sagar et al. (2004) on 4 nights and it showed confirmed INOV each time. It also showed large LTOV, first fading by 0.6 mag over ~ 1 year and then brightening by 1.63 mag on a 2-year time span. In Fig. 2 we present the light curves derived from our newly acquired data on 2 nights. The object showed a clear brightening by 7.5 per cent in 4 hours on 12 Apr 2005. However, on 5 Feb 2005, it remained a non-variable (by the C-test), although a $F-$test showed it to be variable.

- J1058+0133 (PKS 1055+01; $z = 0.888$)

This FSRQ with a variable polarization was a confirmed variable on 2 of the 3 nights we monitored it (Goyal et al. 2011). It also showed a gradual brightening by ~ 0.2 magnitude between 25 Mar. 2007 and 23 Apr. 2007.

- J1159+2914 (4C 29.45; $z = 0.729$)

Confirmed INOV was detected on all the 6 nights this FSRQ was monitored by Noble (1995), with ψ ranging between 4 and 12 per cent (Table 3). It has also shown large variations on *internight* time scales. Firstly, it brightened by 6 per cent between 19 and 21 Jan. 1994 and then faded by $\sim$0.5 mag between 21 and 22 Jan.1994. It again brightened by 7 per cent

between 22 and 23 Jan. 1994 and was last found having faded by $\sim$0.3 mag on the following night.

- J1217+3007 (B2 1215+30; $z = 0.130$)

This blazar was monitored on 4 epochs by Sagar et al. (2004), showing confirmed INOV on 2 epochs (Table 3). Variability was also detected on a longer time scale.

- J1218−0119 (PKS 1216−01; $z = 0.554$)

INOV was detected on all the 4 nights this blazar was monitored by Sagar et al. (2004). On longer time scales, it showed a 2 per cent fading between the first 2 epochs of monitoring, followed by $\sim$ 11 per cent fading over the next 2 days and, finally, 14 per cent brightening within the next 24 hours (Table 3).

- J1310+3220 (B2 1308+32; z = 0.997)

This FSRQ showed a confirmed INOV (ψ up to 3.4 per cent) on one out of the 4 nights it was monitored by Sagar et al. (2004). In the longer term, it showed a strong variability (Stalin et al. 2004a).

- J1510−0906 (PKS 1510-08; $z = 0.360$)

This FSRQ showed confirmed INOV on 2 of the 3 nights it was monitored by us over the span of 5 years (Goyal et al., in prep.). In the long term, it brightened by $\sim$ 1.5 mag over the course of 4 years and then faded by 0.25 mag over the next 19 days when we last monitored it on 20 May 2009. In earlier INOV campaigns by Romero et al. (2002) and Stalin et al. (2005), this blazar was found to be non-variable.

- J2225−0457 (3C 446; $z = 1.404$)

This blazar showed INOV on one of the 2 nights it was monitored by Noble (1995) (Table 3). On 8 Oct 2010 when we monitored it (Goyal et al. 2011), it was found to be non-variable using the $C-$test, but variable by the F-test (Table 3).

- J2253+1608 (3C 454.3; $z = 0.859$)

INOV was detected on both the nights it was monitored by Noble (1995) (Table 3).

5   DISCUSSION

The fairly large size of the TeV blazar sample covered in the present study and the fact that all the key blazar subclasses, namely HBL, IBL, LBL and FSRQ (Sect. 2; Table 1) are included in the sample, reassures us that the INOV results reported here should be representative of TeV blazars. An explicit goal of the present work, the first systematic

study to define the INOV characteristics of TeV blazars, was to search for variations on sub-hour time scales. As pointed out in Sect. 1, TeV blazars are particularly promising targets to look for such ultra-rapid optical continuum variability, since their innermost jets are thought to have extremely large bulk Lorentz factors, $\Gamma \gtrsim 50 - 100$. Despite examining the high-quality intranight monitoring observations of all 22 TeV blazars in our sample, taken on 116 nights over a total duration of 677 hours, no clear event on sub-hour time scales was found, even though the data sampling rate (typically, once every 10 minutes or so) was adequately dense to have revealed any such cases. This demonstrates that the occurrence of optical continuum variability on sub-hour like time scales must be exceedingly rare, at least for amplitudes above ~ 1 per cent, the detection threshold typically reached in the deepest INOV searches made so far. It may nonetheless be noted that our intranight DLCs (Fig. 1) do exhibit a few clear cases of rather sharp "bumps", notably in the cases of J0721+7120 (1 Feb. 2005), J1221+2813 (20 Mar. 2004) and J1256−0547 (26 and 28 Jan. 2006).

As mentioned in Sect. 1, parsec scale radio jets in $\gamma-$ray (EGRET) blazars are known to show faster apparent (superluminal) motion as well as relatively higher brightness temperatures in their cores, compared to non-EGRET blazars (e.g., Kellermann et al. 2004; Jorstad et al. 2001; Taylor et al. 2007; Lister et al. 2009a). Indeed, in an earlier part of our INOV programme, evidence was reported for EGRET detected blazars to exhibit a stronger INOV, again suggesting a link between INOV and the jet speed (Stalin et al. 2005). An independent evidence for such a physical link has emerged in the present study, from a comparison of the INOV duty cycles determined for the two major subclasses of BL Lacs, namely 'low-peaked-BL Lacs (LBL)' and 'high-peaked BL Lacs (HBLs)'. The synchrotron emission from LBLs peaks in the near-infrared/optical domain while for HBLs the synchrotron peak falls in the UV/soft X-ray regime (Urry & Padovani 1995 and references therein). Of the two classes, LBLs are known to display greater activity and this is generally attributed to their emission being dominated by faster jets which are probably also better aligned to our direction (e.g., Ghisellini & Maraschi 1989; Sambruna, Maraschi & Urry 1996; Kharb, Gabuzda & Shastri 2008). Consistent with this picture, it has been found that LBLs display stronger INOV than do HBLs; the duty cycle has been estimated to be $\sim$70 per cent for LBLs and $\sim$30–50 per cent for HBLs (e.g., Romero et al., 1999, 2002; see also, Heidt & Wagner 1998).

The present study allows us to check, for the first time, whether the difference persists even when the two blazar subclasses are subjected to the condition of TeV detection. From Table 1, our sample consists of 7 HBLs (with the lower hump of the SED peaking above 10^{15}

Hz) and 15 other blazars which can be together termed LBLs (see, Abdo et al. 2010b; Li et al. 2010) including J1218−0119 which is a flat-spectrum core dominated quasar. The estimated INOV duty cycles are 38 per cent for HBLs (26 nights' data) and 63 per cent for LBLs (90 nights' data)(Table 3). If only the cases of INOV amplitudes $\psi > 3$ per cent are considered, the duty cycle is 22 per cent for HBLs and 50 per cent for LBLs. Both the estimates for the TeV detected LBLs are in close agreement with those reported in Gopal-Krishna et al. (2003), for radio selected BL Lacs (believed to be predominently LBLs). Figure 4 shows the histograms of INOV DCs for HBLs and LBLs in our sample. The K-S test rejects at the 99 per cent confidence level the hypothesis that the two distributions are drawn from the same parent population. Thus, it is evident that the strong tendency for HBLs to show a milder INOV, vis-á-vis LBLs, persists even if the comaprison is restricted to their TeV detected subsets. This result must be accounted for in physical models of INOV and TeV emission from blazars.

A striking outcome of our search for ultra-rapid INOV is the detection of a curious, sharp feature in the light curve of the HBL J1555+1111 (on 24 June 2009; Fig. 1), the most optically luminous member of Set 1 (Table 1). Intriguingly, instead of being a flare, as is more typical, this essentially symmetric feature is a clear "dip", with an amplitude of ~ 4.2 per cent. Its initial, falling side extends 0.5 hour and the rising side is of a slightly longer duration. We treat this detection as robust, since (i) The profile of the "dip" is well resolved (8 data points); (ii) its peak amplitude is > 20 times the rms noise of individual data points; (iii) the variation is visible with equal clarity and amplitude on the DLCs of the blazar against all the 3 comparison stars; (iv) the 3 comparison stars are all within 0.8 magnitude of the blazar; (v) all 3 comparison stars remained rock-steady through the monitoring duration; and (vi) the atmospheric seeing too remained steady throughout the monitoring session (Fig. 1). All these points, along with the fact that in the DLCs, the brightness levels seen immediately prior to and just after the dip are fairly steady and well matched, *make this feature by far the most credible, if not the only, case of an emission dip (on an hour-like time scale) detected in the optical continuum light received from a blazar.* In addition, the blazar was substantially brighter on both other nights it was monitored by us (Table 3), making it quite unlikely that the elevated flux levels seen just before and after the dip in the light curves of 24 June 2009 are a result of multiple flares occuring at those times.

The robust detection of the dip, combined with its temporal sharpness, calls for an

explanation. A plausible scenario for this rare feature would be that the optical continuum from the jet was temporarily absorbed by a foreground dusty cloud in the nuclear region. An emerging picture of AGN broad emission line clouds suggests they form at the distances from the central continuum source where the temperature becomes low enough for dust formation (i.e., $\sim 10^3$ K) and these dusty clouds then form a dust-driven wind (e.g., Czerny & Hryniewicz 2010; also, Krongold, Binnete & Hernandez-Ibarra 2010). Recalling that the low-level detection (or non-detection) of emission lines in the case of BL Lacs could well be due to a paucity of energetic photons to ionise the gas clouds existing around the central engine (e.g., Ghisellini et al. 2009), it is plausible that a dusty cloud, or a stream of such clouds happens to be on our line of sight to a superluminally moving optical synchrotron 'knot' in the jet. To see if this could explain the "dip", we need an estimate of the size of an optically emitting knot in blazar jets. Here a reasonable expectation would be that optical knots already exist in the jet before the point where the knot becomes visible in the radio band (e.g. Marscher et al. 2008); that point typically occurs at a distance, $l_{rad} \approx 10^3$ times the gravitational radius of the central supermassive black hole (Lobanov 2010). For a typical supermassive black hole of mass $10^8 M_\odot$, the radio visibility point would thus be about $10^{16.5}$ cm away from the nucleus, from which a size of around 10^{15} cm can be reasonably inferred for the optical knot in the jet. The observed time scale of the optical continuum dip ($\sim 10^3$ sec), if interpreted in terms of an occultation of the superluminal knot by a dusty gaseous cloud (see above), would then require a relative transverse speed of order of $30c$ (see Gopal-Krishna & Subramanian 1991 for such a scenario). The corresponding bulk Lorentz factor of the inner jet, $\Gamma \geqslant 30$ for viewing angle $\lesssim 2°$, is not unreasonable for a TeV blazar (Sect. 1). One prediction of this scenario is that any such rapid intensity dips should appear more pronounced in B-band light curves, because of their greater sensitivity to dust obscuration, as compared to the R-band light curves.

Finally, searches for minute-like time scales in the optical light curves of blazars, a key motivation for the present work, have acquired added significance in the present Fermi/LAT era (Atwood et al. 2009). A few recent studies of blazars have revealed a tight physical relationship between $\gamma-$ray and optical flaring events, strongly suggesting a spatial coincidence between their origins, which could well be in the jet's knot crossing a standing shock, located up to several parsecs from the central engine (see, e.g., Agudo et al. 2010, and references therein). More specifically, a recent study of blazars (Ammando et al. 2010) has revealed that polarized optical emission from their jets is spatially coincident with the site of the TeV

flares observed on minute-like time scales. This emerging scenario provides further motivation for more concerted efforts to search for optical variability of TeV blazars on minute-like time scales.

ACKNOWLEDGMENTS

REFERENCES

Abdo A. A., et al., 2009, ApJ, 700, 597

Abdo A. A., et al., 2010a, ApJ, 716, 30

Abdo A. A., et al., 2010b, ApJS, 188, 405

Aharonian F., et al., 2002, A&A, 384, 23

Agudo I., et al., 2010, preprint (astroph/1011.6454v1)

Ammando F. D., 2010, in SciNeGHE 2010 Workshop, September 8-10, 2010, Trieste, Italy. To appear in Il Nuovo Cimento C - Colloquia on physics. preprint (astroph/1012.1120)

Andruchow I., Romero G. E., Cellone S., 2005, A&A, 442, 97

Attridge, J. M., Roberts, D. H., Wardle, J. F. C., 1999, ApJ, 518, L87

Atwood W. B., 2009, ApJ, 697, 1071

Begelman M. C., Blandford R. D., Rees M. J., 1984, RvMP, 56, 255

Begelman M. C., Fabian A. C., Rees M. J., 2008, MNRAS, 384, L19

Bramel D. A., et al., 2005, ApJ, 629, 108

Britzen S., et al., 2008, A&A, 484, 119

Britzen S., et al., 2010, A&A, 515, 105

Carini M. T., Miller H. R., Goodrich B. D., 1990, AJ, 100, 347

Cellone S. A., Romero G. E., Combi J. A., 2000, AJ, 119, 1534

Cellone S. A., Romero G. E., Araudo A. T., 2007, MNRAS, 374, 357

Ciprini S., et al, 2007, A&A, 467, 465

Chen Y., Gu M., Shen Z.-Q., Fan Z., 2006, MNRAS, 370, 1885

Costamante L., et al., 2001, A&A, 371, 512

Costamante L., Aharonian F., Buehler R., Khangulyan D., Reimer A., Reimer O., 2009, preprint (astroph/0907.3966)

Czerny B., Hryniewicz K., preprint (astroph/1010.6201)

Dai B. Z., Xie G. Z., Li K. H., Zhou S. B., Liu W. W., Jiang Z. J., 2001, AJ, 122, 2901

de Diego J. A., 2010, AJ, 139, 1269

Edelson R., Turner T. J., Pounds K., Vaughan S., Markowitz A., Marshall H., Dobbie P., Warwick R., 2002, ApJ, 568, 610

Fabian A. C., Rees M. J., 1979, MNRAS, 187

Fan J. H., Cheng K. S., Zhang L., Liu C. H., 1997, A&A, 327, 947

Giannios D., Uzdensky D. A., Begelman M. C., 2009, MNRAS, 395, 29

Ghisellini G., Haardt F., Matt G, 2004, A&A, 413, 523

Ghisellini G., Maraschi, L., 1989, ApJ, 340, 181

Ghisellini G., et al., 1997, A&A, 327, 61

Ghisellini G., Maraschi, L., Tavecchio, F. 2009, MNRAS, 396, L105

Giroletti M., Giovannini G., Taylor G. B., Falomo R., 2004, ApJ, 613, 752

Giroletti M., Giovannini G., Taylor G. B., Falomo R., 2006, ApJ, 646, 801

Gopal-Krishna, Singal, A.K., Krishnamohan, S., 1984, A&A, 140, L19

Gopal-Krishna, Subramanian K., 1991, Nature, 349, 766

Gopal-Krishna, Stalin C. S., Sagar R., Wiita P. J., 2003, ApJ, 586, L25

Gopal-Krishna, Dhurde, S., Wiita P. J., 2004, ApJL, 615, L81

Gopal-Krishna, Wiita P. J., Dhurde S., 2006, MNRAS, 369, 1281

Gopal-Krishna, Dhurde S., Sirkar P., Wiita P. J., 2007, MNRAS, 377, 446

Goyal A., et al., 2009, MNRAS, 399, 1622

Goyal A., Gopal-krishna, Wiita P. J. W., Anupama G. C., Sahu D. K. S., Sagar R., 2011,
 submitted

Guilbert P. W., Fabian A. C., Rees M. J., 1983, MNRAS, 205, 593

Gupta A. C., Fan J. H., Bai J. M., Wagner S. J., 2008, AJ, 135, 1384

Hartman R. C., et al., 1992, ApJL, 385, 1

Heidt J., Wagner S. J., 1998, A&A, 329, 853

Helmboldt J. F., et al., 2007, ApJ, 658, 203

Impiombato D., et al., 2011, ApJS, 192, 12

Jannuzi B. T., Smith P. S., Elston R., 1993, ApJS, 85, 265

Jorstad S. G., Marscher A. P., Mattox J. R., Wehrle A. E., Bloom S. D., Yurchenko A. V.,
 2001, ApJS, 134, 181

Kataoka J., et al., 2001, ApJ, 560, 659

Kellermann K. I., Pauliny-Toth I. I. K., 1969, ApJ, 155, 71

Kellermann K. I., et al., 2004, ApJ, 609, 539

Kharb P., Gabuzda D., Shastri P., 2008, MNRAS, 384, 230

Kidger M. R., deDiego, J. A., 1990, A&A, 227, L25

Kovalev Y. Y., Nizhelsky N. A., Kovalev Y. A., Berlin A. B., Zhekanis G. V., Mingaliev
 M. G., Bogdantsov A. V., 1999, A&AS, 139, 545

Kovalev Y. Y., et al., 2005 AJ, 130, 2473

Kovalev Y. Y, et al., 2009 ApJL, 696, 17

Krawczynski H., Coppi P. S., Aharonian F., 2002, MNRAS, 336, 721

Krongold Y., Binette L., Hernandez-Ibarra F., 2010, ApJ, 724 L203

Kundt W., Gopal-Krishna, 1980, Nature, 288, 149

Kundt W., Gopal-Krishna, 2004, JApA, 25, 115

Li H. Z., Xie G. Z., Yi T. F., Chen L. E., Dai H., 2010, ApJ, 709, 1407

Lister M. L., Homan D. C., 2005, ApJL, 130, 1389

Lister M. L., Homan D. C., Kedler M., Kellermann K. I., Kovalev Y. Y., Ros E., Savolainen T., Zensus A., 2009a, ApJL, 696, 22

Lister M. L., et al., 2009b, AJ, 138, 1874

Lobanov A.P., in "Steady jets and transient jets", Bonn, 7-8 April 2010. published in Memorie della Societa Astronomica Italiana, v.81, n.4 (2010)

MAGIC collaboration; Albert J., et al., 2008, Science, 320, 1752

Marscher A. P., 1996, in Blazar continuum variability, eds. H.R. Miller, J.R. Webb, and J.C. Noble, ASP Conf. Ser. Vol. 110, (San Francisco: ASP), p. 248

Marscher A. P., Jorstad S. G., Mattox J. R., Wehrle A. E., 2002, ApJ, 577, 85

Marscher, A.P. et al. 2008, Nature, 452, 966

Mihov B., Bachev R., Slavcheva-Mihova L., Strigachev A., Semkov E., Petrov G., 2008, AN, 329, 77

Monet D. G., et al., 2003, AJ, 125, 984

Noble J. C., 1995, PhD thesis, Georgia State University

Perri M., et al., 2003, 407, 453

Petrucci P. O., Boutelier T., Henri G., 2010, preprint (astroph/1010.5895)

Piner B. G., Edwards P. G., 2004, ApJ, 600, 115

Piner B. G., Pant N., Edwards P. G., 2008, ApJ, 678, 64

Pollock J. T., Webb J. R., Azarnia G., 2007, ApJ, 133, 487

Rani, B., Gupta, A.C., Joshi, U.C., Ganesh, S., Wiita, P.J., 2010, ApJ, 719, L153

Rector T. A., Gabuzda D. C., Stocke J. T., 2003, AJ, 125, 1060

Romero G. E., Cellone S. A., Combi J. A., 1999, A&AS, 135, 477

Romero G. E., Cellone, S. A., Combi J. A., Andruchow I., 2002, A&A, 390, 431

Sagar R., 1999, Curr. Sci, 77, 643

Sagar R., Gopal-Krishna, Mohan V., Pandey A. K., Bhatt B. C., Wagner S.J., 1999, A&AS, 134, 453

Sagar R., Stalin C. S., Gopal-Krishna, Wiita P. J., 2004, MNRAS, 348, 176

Sambruna R. M., Maraschi L., Urry C. M. 1996, ApJ, 463, 444

Savolainen T., Homan D. C., Hovatta T., Kadler M., Kovalev Y. Y., Lister M. L., Ros E., Zensus J. A., 2010, A&A, 512, 24

Schlegel D. J., Finkbeiner D. P., Davis M., 1998, ApJ, 500, 525

Schlickeiser R., 1996, A&AS, 120, 481

Spergel D. N., 2007, ApJS, 170, 377

Stalin C. S., Gopal-Krishna, Sagar R., Wiita P. J., 2004a, JApA, 25, 1

Stalin, C. S., Gopal-Krishna, Sagar, R., Wiita, P. J., 2004b, MNRAS, 350, 175

Stalin C. S., Gupta A. C., Gopal-Krishna, Wiita P. J., Sagar R., 2005, MNRAS, 356, 607

Stetson P. B., 1987, PASP, 99, 191

Stocke J. T., Foltz C. B., Weymann R. J., Christiansen W. A., 1984, ApJ, 280, 476

Stockman H. S., Moore R. L., Angel J. R. P., 1984, ApJ, 279, 485

Takalo L. O., Sillanpää A., Nilsson K., 1994, A&AS, 107, 497

Stocke J. T., Morris S. L., Weymann R. J., Foltz C. B., 1992, ApJ, 396, 487

Tanihata C., Urry C. M., Takahashi T., Kataoka J., Wagner S. J., Madejski G. M., Tashiro M., Kouda M., 2001, ApJ, 563, 569

Taylor G. B., et al., 2007 ApJ, 671, 1355

Treves A., Falomo R., Uslenghi M., 2007, A&A, 473, 17

Urry C. M., Padovani P., 1995, PASP, 107, 803

Véron-Cetty M.-P.; Véron P., 2006, A&A, 455, 773

Visvanathan N., Wills B. J., 1998, AJ, 116, 2119

Wagner S. J., Witzel A., 1995, ARA&A, 33, 163

Wagner S. J., et al., 1996, AJ, 111, 2187

Webb W., Malkan M., 2000, ApJ, 540, 652

Weekes T. C., 2008, in High Energy Gamma-Ray Astronomy, Ed. F. A. Aharonian, W. Hofmann & F. Rieger, AIP Conf. Ser., 1085, 3

Wehrle A. E., Morabito D. D., Preston R. A., 1984, ApJ, 89, 336

Wiita P. J., 2006, in Blazar Variability Workshop II: Entering the GLAST Era ASP Conference Series, Vol. 350, eds. H. R. Miller, K. Marshall, J. R. Webb, and M. F. Aller. (San Francisco: ASP), p. 183

Wills B. J., Wills D., Breger M., Antonucci R. R. J., Barvianis R., 1992, ApJ, 398, 454

Xie G. Z., Li K. H., Bai J. M., Dai B. Z., Liu W. W., Zhang X., Xing S. Y., 2001, ApJ, 548, 200

Table 1. The sample of 22 TeV blazars studied in the present work

IAU name (1)	Other name (2)	Type (3)	R.A.(J2000) (h m s) (4)	Dec(J2000) (° ′ ″) (5)	B (6)	M_B (7)	z (8)	P_{op}(%) (9)	α_r (10)	P_c^{5GHz} (W/Hz) (11)	P_{ext}^{5GHz} (W/Hz) (12)	$\log f_c$ (13)	$\log R^*$ (14)	β_{app} (max) (15)
Set 1														
J0222+4302	3C 66A	IBL	02 22 39.6	+43 02 08	15.71	−24.96	0.444	16.8^a	$-0.20^§$	$6.5 \times 10^{26\,h}$	1.1×10^{27}	-0.22	2.98	5.8^n
J0721+7120	S5 0716+71	IBL	07 21 53.3	+71 20 36	15.50	−24.73	0.310	29.0^b	$+0.36$	$1.0 \times 10^{27\,i}$	4.5×10^{26}	0.36	2.43	10.07^o
J0809+5218	1ES 0806+524	HBL	08 09 49.2	+52 18 58	15.30	−23.25	0.138		-0.25	$5.6 \times 10^{24\,j}$	2.7×10^{24}	0.30	1.79	
J1015+4926	GB 1011+496	HBL	10 15 04.2	+49 26 01	16.56	−22.88	0.200		-0.26	$2.0 \times 10^{25\,k}$	1.8×10^{25}	0.03	2.59	
J1221+3010	PG 1218+304	HBL	12 21 21.9	+30 10 37	16.50	−22.72	0.182	6.6^e	-0.08	$5.4 \times 10^{24\,j}$	1.3×10^{24}	0.58	1.85	
J1221+2813	ON 231	HBL	12 21 31.7	+28 13 58	16.81	−21.21	0.102	4.3^e	$-0.09^§$	$1.5 \times 10^{25\,i}$	3.1×10^{24}	0.70	3.01	3.2^q
J1256−0547	3C 279	FSRQ	12 56 11.1	−05 47 21	18.01	−23.24	0.538	44.0^b	$+0.48^§$	$3.2 \times 10^{28\,i}$	1.0×10^{28}	0.50	4.51	20.58^o
J1428+4240	H 1426+428	HBL	14 28 32.7	+42 40 21	16.95	−21.60	0.129	2.5^d	-0.58	$1.5 \times 10^{24\,j}$	7.2×10^{23}	0.34	1.96	2.09^r
J1555+1111	PG 1553+11	HBL	15 55 43.1	+11 11 24	15.00	−25.42	$0.360^‡$	3.5^g	$+0.54$	$1.5 \times 10^{26\,m}$	1.9×10^{25}	0.88	1.85	
Set 2														
J0238+1637	AO 0235+164	LBL	02 38 38.9	+16 37 00	16.46	−25.47	0.940	43.9^b	$+0.71^§$	$1.3 \times 10^{28\,i}$	2.1×10^{27}	0.80	3.12	
J0423−0120	PKS 0420-01	FSRQ	04 23 15.8	−01 20 33	17.50	−24.17	0.915	20.0^b	$+0.19^§$	$8.2 \times 10^{28\,i}$	4.4×10^{28}	0.27	3.69	7.35^o
J0738+1742	PKS 0735+17	LBL	07 38 07.4	+17 42 19	16.76	−24.04	>0.424	36.0^b	$-0.28^§$	$1.5 \times 10^{27\,i}$	3.6×10^{26}	0.61	3.40	11.8^p
J0739+0137	PKS 0736+01	FSRQ	07 39 18.0	+01 37 04	16.90	−21.96	0.191	5.6^c	$-0.10^§$	$2.2 \times 10^{26\,i}$	1.3×10^{25}	1.20	3.45	14.44^o
J0854+2006	OJ 287	LBL	08 54 48.8	+20 06 30	15.91	−24.30	0.306	37.2^b	$+0.20^§$	$1.6 \times 10^{27\,i}$	6.2×10^{26}	0.41	2.91	11.70^o
J1058+0133	PKS 1055+01	FSRQ	10 58 29.6	+01 33 58	18.74	−23.34	0.888	5.0^d	$+0.06^§$	$3.9 \times 10^{28\,i}$	1.1×10^{28}	0.54	4.26	11.0^o
J1159+2914	4C 29.45	FSRQ	11 59 31.9	+29 14 45	14.80	−27.00	0.729	28.0^b	$-0.34^§$	$1.3 \times 10^{28\,i}$	3.6×10^{27}	0.57	2.60	24.8^o
J1217+3007	B2 1215+30	HBL	12 17 52.0	+30 07 01	16.07	−22.45	0.130	8.0^e	$-0.12^§$	$1.3 \times 10^{25\,j}$	8.8×10^{24}	0.17	2.60	
J1218−0119	PKS 1216-010	$BL^£$	12 18 34.9	−01 19 54.0	16.17	−25.14	0.554	6.9^f	$+0.01^§$	$4.3 \times 10^{27\,l}$	2.5×10^{27}	0.22	3.01	
J1310+3220	B2 1308+32	FSRQ	13 10 28.7	+32 20 44	15.61	−26.69	0.997	28.0^b	$-0.09^§$	$3.0 \times 10^{28\,i}$	9.9×10^{27}	0.49	2.71	27.2^o
J1512−0906	PKS 1510-08	FSRQ	15 12 50.5	−09 06 00	16.74	−23.49	0.360	7.8^b	$-0.10^§$	$1.7 \times 10^{27\,i}$	7.7×10^{25}	1.35	3.48	20.2^o
J2225−0457	3C 446	FSRQ	22 25 47.2	−04 57 01	18.83	−23.66	1.404	17.3^b	$-0.13^§$	$1.3 \times 10^{29\,i}$	6.2×10^{28}	0.34	4.58	17.34^o
J2253+1608	3C 454.3	FSRQ	22 53 57.7	+16 08 53	16.57	−25.11	0.859	16.0^b	$-0.28^§$	$6.7 \times 10^{28\,i}$	1.2×10^{28}	0.74	3.99	14.19^o

Columns: (1) source name; (2) most popular name as given in Véron & Véron (2006); (3) classification into low-, intermediate-, or high-frequency peaked blazars or flat spectrum radio quasar (FSRQ); (4) right ascension; (5) declination; (6) apparent B-magnitude; (7) absolute B-magnitude; (8) redshift; (9) the measured optical polarization; (10) radio spectral index; (11) radio core luminosity; (12) extended emission radio luminosity; (13) radio core dominance parameter f_c (see text); (14) radio loudness R^*; (15) the fastest apparent speed observed in the parsec-scale jet (in units of the speed of light).

Footnotes :
Column 3 : Abdo et al. (2010a), $^£$ SED classification is not available.
Column 8 : ‡ reference for redshift: Rector et al. (2003), see also, Treves, Falomo & Uslenghi (2007)
Column 9 : (a) Takalo, Silanpää & Nilsson (1994); (b) Fan et al. (1997); (c) Stockman, Moore & Angel (1984); (d) Jannuzi, Smith & Elston (1993) ; (e) Wills et al. (1992); (f) Visvanathan & Wills (1998); (g) Andruchow, Romero & Cellone (2005).
Column 10 : § is the radio spectral index derived using simultaneous flux measurements from Kovalev et al. (1999) by means of least square method ($S_\nu \propto \nu^\alpha$). The remaining values of α_r have been calculated using 6 and 20 cm. flux densities from Véron & Véron (2006).
Column 11 : Reference for VLBI flux: (h) Marscher et al. (2002); (i) Kovalev et al. (2005); (j) Giroletti et al. (2006); (k) Helmboldt et al. (2007); (l) Wehrle, Morabito & Preston (1984); (m) Rector et al. (2003).
Column 14 : R^* is the K-corrected rest frame ratio of the 5 GHz to 2500 Å flux densities, following Stocke et al. (1992); reference for the radio flux is Véron & Véron (2006).
Column 15 : Reference for β_{app}: (n) Britzen et al. (2008); (o) Lister et al. (2009b); (p) Britzen et al. (2010); (q) Kellermann et al. (2004); (r) Piner et al. (2008).

Table 2. Positions and apparent magnitudes* of the TeV blazars and the comparison stars.

Source	Set No.	R.A.(J2000) (h m s)	Dec(J2000) (° ′ ″)	B* (mag)	R* (mag)	B-R (mag)
J0222+4302	1	02 22 39.61	+43 02 07.9	14.94	14.35	0.59
S1		02 22 28.41	+43 03 40.9	14.59	14.00	0.59
S2		02 22 20.45	+42 57 18.7	14.74	13.66	1.08
S3		02 22 39.09	+42 57 05.5	14.69	13.94	0.75
J0238+1637	2	02 38 38.92	+16 36 59.2	18.65	15.92	2.73
S1		02 38 56.00	+16 37 43.0	17.43	16.60	0.83
S2		02 38 38.52	+16 40 05.3	18.37	16.61	1.76
S3		02 38 22.25	+16 39 41.8	17.37	16.22	1.15
J0721+7120	1	07 21 53.39	+71 20 36.7	15.15	14.27	0.88
S1		07 22 12.58	+71 21 15.2	14.49	13.78	0.71
S2		07 21 54.31	+71 19 21.2	14.46	13.67	0.79
S3		07 21 13.95	+71 17 10.0	14.45	13.55	0.90
J0809+5218	1	08 09 49.20	+52 18 58.4			
S1		08 09 43.90	+52 18 09.5	16.17	15.47	0.70
S2		08 10 16.45	+52 19 16.9	17.85	16.10	1.75
S3		08 09 52.68	+52 16 15.1	15.25	14.73	0.52
J1015+4926	1	10 15 04.13	+49 26 00.8	15.32	14.58	0.74
S1		10 15 29.71	+49 30 41.5	15.27	14.84	0.43
S2		10 15 37.87	+49 28 19.2	14.92	14.56	0.36
S3		10 15 08.03	+49 25 42.3	14.27	13.55	0.72
S4		10 15 39.84	+49 29 25.7	16.70	14.95	1.75
J1221+3010	1	12 21 21.93	+30 10 37.2	16.13	14.93	1.20
S1		12 21 22.62	+30 09 53.8	16.72	15.43	1.29
S2		12 21 23.08	+30 10 38.9	17.04	15.42	1.62
S3		12 21 37.05	+30 10 18.3	16.28	15.52	0.76
J1221+2813	1	12 21 31.69	+28 13 58.4	14.65	14.24	0.41
S1		12 21 26.01	+28 12 30.9	16.94	15.91	1.03
S2		12 21 13.86	+28 13 04.5	13.61	12.88	0.73
S3		12 21 11.81	+28 11 53.7	16.13	15.00	1.13
J1256−0547	1	12 56 11.19	−05 47 21.5	17.39	15.87	1.52
S1		12 56 26.61	−05 45 22.8	15.22	14.75	0.47
S2		12 55 58.00	−05 44 18.9	16.19	15.30	0.89
S3		12 56 14.48	−05 46 47.8	16.39	15.43	0.96
J1428+4240	1	14 28 32.62	+42 40 21.4			
S1		14 28 08.06	+42 40 37.4	16.62	16.23	0.39
S2		14 28 07.38	+42 44 20.0	16.16	15.74	0.42
S3		14 28 16.05	+42 40 39.9	16.77	16.56	0.21
J1555+1111	1	15 55 43.05	+11 11 24.3	14.30	13.99	0.31
S1		15 55 46.08	+11 11 19.6	14.52	13.62	0.90
S2		15 55 52.17	+11 13 18.5	14.47	13.56	0.91
S3		15 55 40.77	+11 04 44.7	14.46	13.56	0.90
S4		15 56 06.02	+11 13 44.9	15.44	14.54	0.90
J0854+2006	2	08 54 48.68	+20 06 30.8	15.95	15.56	0.40
S1		08 54 53.36	+20 04 45.1	15.25	13.97	1.28
S2		08 54 41.29	+20 06 43.2	16.86	15.60	1.26
S3		08 54 55.19	+20 05 42.4	15.83	14.94	0.89

*Monet et al. (2003)

Table 3. Summary of observations and INOV results

Source	Set No.	Epoch dd.mm.yy	Tel. used	Fil.	Dur. (hours)	N_{points}	σ (%)	ψ (%)	C_{eff}	Status[†] (C-test)	F-value(DoF[‡])	Status[†] (F-test)	Ref.[£]
(1)	(2)	(3)	(4)	(5)	(6)	(7)	(8)	(9)	(10)	(11)	(12)	(13)	(14)
J0222+4302	1	14.11.98	ST	R	6.5	118		5.4	6.0	V			(a)
		13.11.99	ST	R	5.7	123		5.5	>6.6	V			(a)
		24.10.00	ST	R	9.1	73		4.3	5.8	V			(a)
		26.10.00	ST	R	10.1	82		3.2	3.5	V			(a)
		01.11.00	ST	R	9.0	103		2.2	2.9	V			(a)
		24.11.00	ST	R	5.1	71				N			(a)
		01.12.00	ST	R	5.1	59		8.0	>6.6	V			(a)
		27.09.09	ST	R	4.1	34	0.28	1.0	1.6	N	1.15(33)	N	(b)
		28.09.09	ST	R	6.2	38	0.19	1.1	2.6	V	3.75(37)	V	(b)
J0238+1637	2	27.10.90		V	4.5		1.00	5.0		V			(c)
		29.10.90		V	8.3		1.20	18.0		V			(c)
		05.11.91		R	6.3		1.20	20.0		V			(c)
		07.11.91		R	8.0		1.20	5.0		V			(c)
		08.11.91		R	9.4		1.30	16.0		V			(c)
		03.11.99		V	6.7		1.40	27.3	10.0	V			(d)
		04.11.99		V	6.6		1.20	24.5	6.1	V			(d)
		05.11.99		V	7.0		1.20	34.5	8.9	V			(d)
		06.11.99		V	6.7		0.70	11.0	4.4	V			(d)
		07.11.99		V	6.6		0.90	44.3	14.4	V			(d)
		12.11.99	ST	R	6.6	39		12.8	6.6	V			(a)
		14.11.99	ST	R	6.2	34		10.2	3.2	V			(a)
		22.10.00	ST	R	7.9	39		7.6	2.6	V			(a)
		22.12.00		V	7.2		0.70	7.0	3.3	V			(d)
		18.11.03	HCT	R	7.4	39	0.40	6.8	>5.54	V	58.71(38)	V	(e)
J0423−0120	2	19.11.03	ST	R	6.3	36	0.25	1.6	3.60	V	7.81(35)	V	(e)
		08.12.04	ST	R	6.0	11	0.26	1.8	0.96	N	10.51(10)	V	(e)
		25.10.09	ST	R	4.0	18	0.38	2.9	2.00	PV	6.45(17)	V	(e)
J0721+7120	1	23.03.04		R	7.0			6.0		V			(f)
		01.02.05	ST	R	1.5	24	0.25	3.1	5.1	V	22.15(23)	V	(b)
		12.01.07		R	3.6	185	0.70	6.3	2.8	V			(g)
		20.03.07		R	4.2	195	0.50		1.6	N			(g)
J0738+1742	2	26.12.98	ST	R	7.8	49		1.8	1.13	N			(a)&(h)
		30.12.99	ST	R	7.4	64		1.0	0.61	N			(a)&(h)
		25.12.00	ST	R	6.0	42		1.6	1.02	N			(a)&(h)
		25.12.01	ST	R	7.3	43		1.0	2.8	V			(a)&(h)
		20.12.03	HCT	R	5.8	36	0.23	1.0	1.78	N	1.86(35)	N	(h)
		10.12.04	ST	R	5.8	28	0.16	1.3	3.00	V	8.40(27)	V	(h)
		23.12.04	ST	R	5.0	11	0.10	1.2	3.10	V	17.83(10)	V	(h)
		02.01.05	ST	R	4.9	20	0.22	0.8	0.97	N	1.42(19)	N	(h)
		05.01.05	ST	R	5.8	23	0.15	1.0	2.25	PV	7.00(22)	V	(h)
		09.01.05	ST	R	6.7	28	0.19	1.3	3.20	V	9.78(27)	V	(h)
		09.11.05	ST	R	3.8	17	0.17	0.7	2.00	PV	3.35(16)	PV	(h)
		16.11.06	ST	R	4.5	19	0.29	1.1	0.95	N	4.35(18)	V	(h)
		29.11.06	ST	R	5.8	26	0.19	1.0	0.83	N	3.42(25)	V	(h)
		17.12.06	ST	R	5.6	24	0.19	0.9	1.06	N	5.72(23)	V	(h)
		15.12.07	ST	R	6.6	28	0.29	1.9	3.53	V	10.37(27)	V	(h)
		16.12.07	ST	R	6.6	27	0.19	1.0	1.45	N	3.87(26)	V	(h)
		22.11.08	ST	R	5.6	27	0.19	0.8	0.33	N	1.84(26)	N	(h)
J0739+0137	2	05.12.05	HCT	R	5.3	10	0.38	3.4	2.93	V	36.84(9)	V	(e)
		06.12.05	HCT	R	6.0	09	0.54	3.1	3.50	V	6.23(8)	V	(e)
		09.12.05	HCT	R	5.5	14	0.54	1.3	0.38	N	1.45(13)	N	(e)
J0809+5214	1	04.02.05	HCT	R	6.8	27	0.20	1.2	2.31	PV	1.86(26)	N	(b)
		05.12.05	HCT	R	4.3	08	0.24	0.8	0.59	N	3.40(7)	N	(b)
		08.12.05	HCT	R	4.9	14	0.11	0.4	0.15	N	1.45(13)	N	(b)
		09.12.05	HCT	R	4.8	12	0.24	0.5	0.32	N	1.27(11)	N	(b)

Table 3 (cont'd)

Source	Set No.	Epoch dd.mm.yy	Tel. used	Fil.	Dur. (hours)	N_{points}	σ (%)	ψ (%)	C_{eff}	Status† (C-test)	F-value(DoF‡)	Status† (F-test)	Ref.£
(1)	(2)	(3)	(4)	(5)	(6)	(7)	(8)	(9)	(10)	(11)	(12)	(13)	(14)
J0854+2006	2	29.12.98	ST	R	6.8	19		2.3	2.80	V			(a)
		31.12.99	ST	R	5.6	29		3.8	6.50	V			(a)
		28.03.00	ST	R	4.2	22		5.0	5.80	V			(a)
		17.02.01	ST	R	6.9	48		2.8	2.70	V			(a)
		05.02.05	HCT	R	7.7	40	0.23	0.8	1.69	N	2.57(39)	V	(b)
		12.04.05	ST	R	4.1	54	0.32	7.5	5.20	V	71.39(54)	V	(b)
J1015+4926	1	06.02.10	ST	R	5.5	24	0.25	1.0	0.98	N	2.08(23)	N	(b)
		19.02.10	ST	R	5.6	41	0.30	1.8	2.17	PV	5.06(40)	V	(b)
		07.03.10	ST	R	5.2	34	0.36	3.4	4.30	V	11.99(33)	V	(b)
J1058+0133	2	25.03.07	ST	R	5.8	11	0.12	2.0	3.20	V	58.56(10)	V	(e)
		16.04.07	ST	R	3.8	15	0.17	0.8	0.53	N	1.37(14)	N	(e)
		23.04.07	ST	R	4.4	10	0.23	1.8	2.57	V	12.51(9)	V	(e)
J1159+2914	2	19.01.94		R	4.0		0.90	12.0		V			(c)
		20.01.94		R	5.5		0.80	3.0		V			(c)
		21.01.94		R	5.1		0.90	10.0		V			(c)
		22.01.94		R	5.4		1.10	11.0		V			(c)
		23.01.94		R	5.1		1.00	4.0		V			(c)
		24.01.94		R	4.0		1.30	7.0		V			(c)
J1217+3007	2	20.03.99	ST	R	7.0	21		3.50	5.50	V			(a)
		25.02.00	ST	R	5.9	28				N			(a)
		31.03.00	ST	R	5.0	27				N			(a)
		19.04.02	ST	R	6.8	23		1.80	4.90	V			(a)
J1218−0119	2	11.03.02	ST	R	8.0	22		7.3	3.20	V			(a)
		13.03.02	ST	R	8.5	24		3.8	2.60	V			(a)
		15.03.02	ST	R	3.9	11		5.5	3.50	V			(a)
		16.03.02	ST	R	8.2	22		14.1	>5.54	V			(a)
J1221+3010	1	08.03.10	IGO	R	6.2	15	0.24	0.9	1.18	N	1.96(14)	N	(b)
		18.03.10	ST	R	4.7	25	0.49	1.0	0.26	N	2.12(24)	N	(b)
		22.05.10	ST	R	3.9	19	0.88	3.3	0.41	N	2.23(18)	PV	(b)
J1221+2813	1	19.03.04	HCT	V	5.4	74	0.32	5.2	>5.54	V	16.65(72)	V	(b)
		20.03.04	HCT	V	6.6	97	0.49	8.2	>5.54	V	62.42(96)	V	(b)
		18.03.05	ST	R	4.0	26	0.33	2.0	1.74	N	3.21(25)	V	(b)
		05.04.05	ST	R	6.9	38	0.20	3.2	4.50	V	27.71(37)	V	(b)
J1256−0547	1	26.01.06	ST	R	4.2	19	0.17	2.5	>5.54	V	13.59(18)	V	(b)
		28.02.06	ST	R	6.1	40	0.25	10.2	>5.54	V	403.89(39)	V	(b)
		20.04.09	ST	R	4.9	20	0.44	22.0	>5.54	V	1069.51(19)	V	(b)
J1310+3220	2	26.04.00	ST	R	5.6	16				N			(a)
		17.03.02	ST	R	7.7	19		3.4	3.1	V			(a)
		24.04.02	ST	R	5.8	14				N			(a)
		02.05.02	ST	R	5.1	15				N			(a)
J1428+4240	1	21.04.04	HCT	V	5.8	32	0.46	2.8	1.82	N	2.90(31)	V	(b)
		22.04.09	ST	R	4.0	16	0.37	1.1	0.28	N	1.99(15)	N	(b)
		29.04.09	ST	R	6.4	27	0.73	2.1	0.65	N	1.42(26)	N	(b)
J1512−0906	2	28.04.98		V	3.8		0.30			N			(i)
		29.04.98		V	4.0		0.40			N			(i)
		30.04.98		V	4.0		0.80	4.2	1.45	N			(d)
		06.06.99		V	7.2		0.90	3.4	1.05	N			(d)
		07.06.99		V	7.3		0.90	4.2	1.27	N			(d)
		14.06.05	ST	R	4.0	09	0.12	1.6	1.53	N	12.02(8)	V	(e)
		01.05.09	ST	R	5.6	22	0.31	4.7	2.63	V	29.85(21)	V	(e)
		20.05.09	ST	R	4.8	23	0.43	3.1	0.98	N	4.20(22)	V	(e)

Table 3 (cont'd)

Source	Set No.	Epoch dd.mm.yy	Tel. used	Fil.	Dur. (hours)	N_{points}	σ (%)	ψ (%)	$C_{\rm eff}$	Status[†] (C-test)	F-value(DoF[‡])	Status[†] (F-test)	Ref.[£]
(1)	(2)	(3)	(4)	(5)	(6)	(7)	(8)	(9)	(10)	(11)	(12)	(13)	(14)
J1555+1111	1	05.05.99	ST	R	3.6	20		2.3	>6.60	V			(i)
		06.06.99	ST	R	7.1	40				N			(i)
		24.06.09	ST	R	3.8	23	0.17	4.2	>5.54	V	50.81(22)	V	(b)
		15.05.10	ST	R	6.1	25	0.29	2.8	>5.54	V	12.99(24)	V	(b)
		16.05.10	ST	R	6.1	31	0.30	2.3	4.63	V	6.33(30)	V	(b)
J2225−0457	2	29.09.88		R	4.8		0.80	9.0		V			(c)
		01.10.88		R	6.7		0.90			N			(c)
		08.10.10		R	5.1	16	0.64	6.8	1.12	N	14.35(15)	V	(e)
J2253+1608	2	12.09.90		R	6.9		1.00	6.0		V			(c)
		13.09.90		R	7.5		1.10	4.0		V			(c)

[†] V= variable, N = non-variable, PV = probable variable

[‡] DOF = degrees of freedom

[£] Reference for INOV data: (a) Sagar et al. (2004); (b) Present work; (c) Noble (1995); (d) Romero et al. (2002); (e) Goyal et al. (2011) (f) Pollock, Webb & Azarnia (2007); (g) Gupta et al. (2008); (h) Goyal et al. (2009); (i) Stalin et al. (2005)
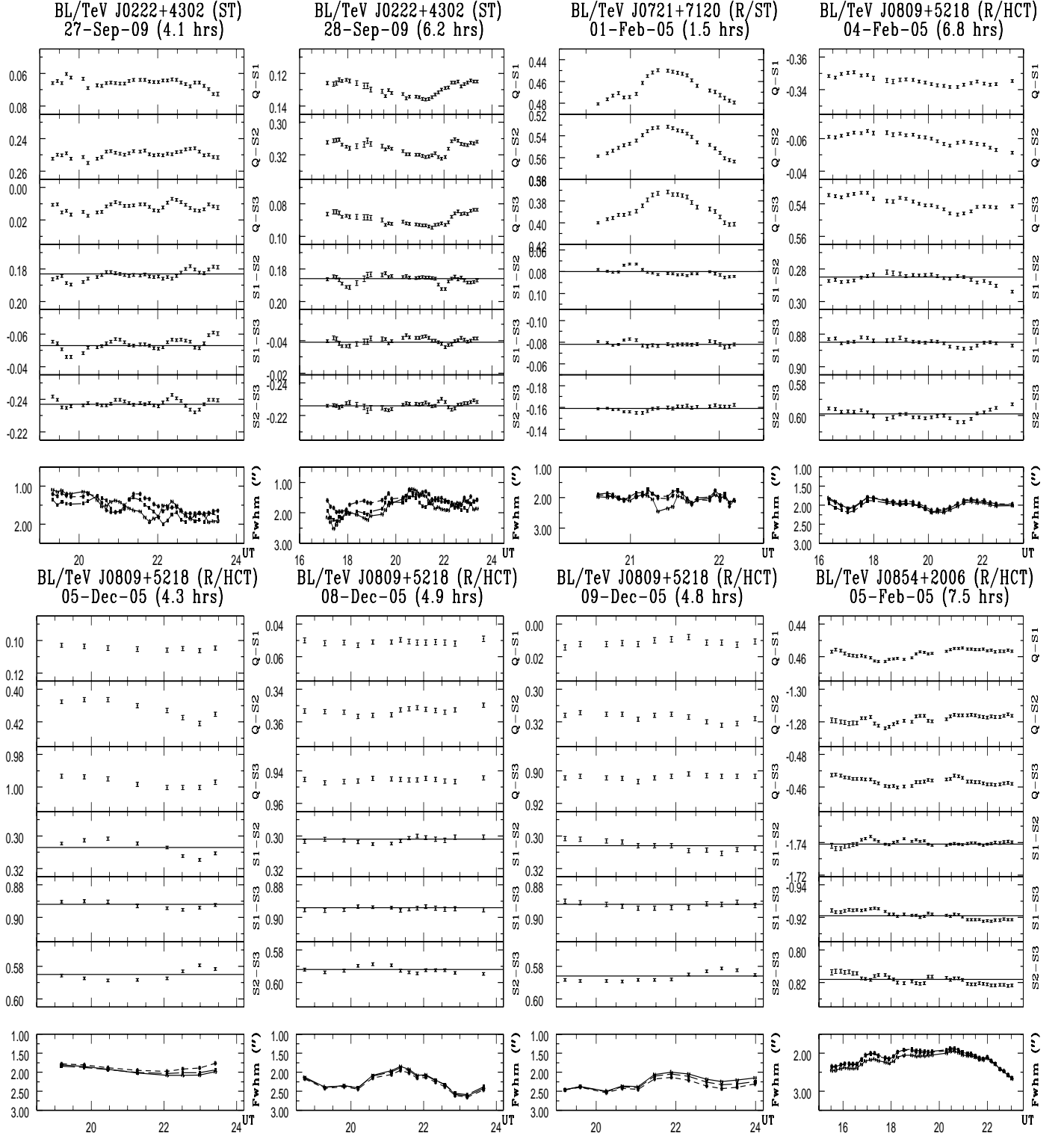
Figure 1. Intranight DLCs of the 9 TeV blazars (Set 1) and J0854+2006 (Set 2) monitored in the present study. The source name, date of monitoring, its duration, the filter and the telescope used are mentioned at the top of each frame. For each night the bottom panel shows the variation of the atmospheric seeing through the monitoring duration.
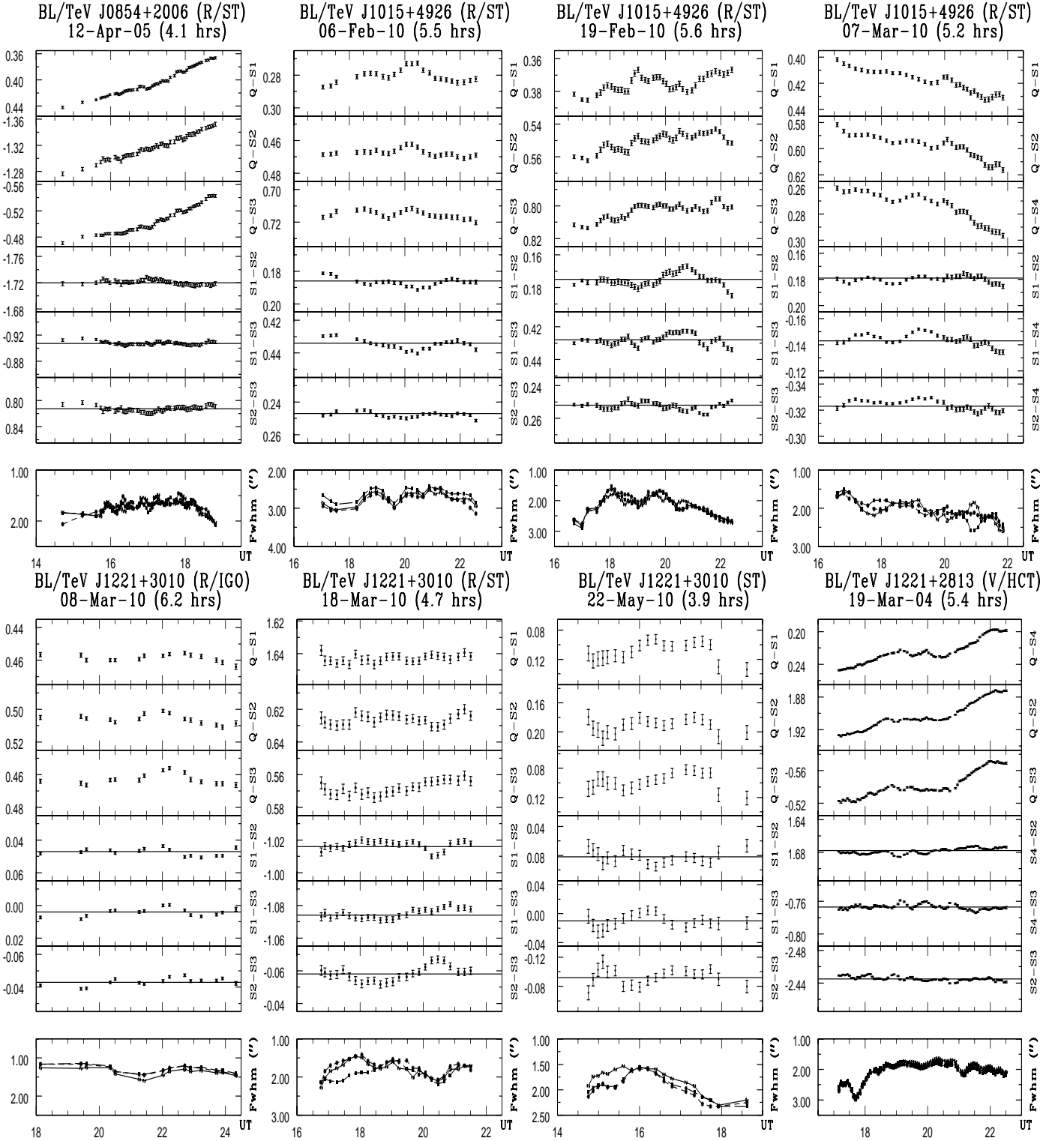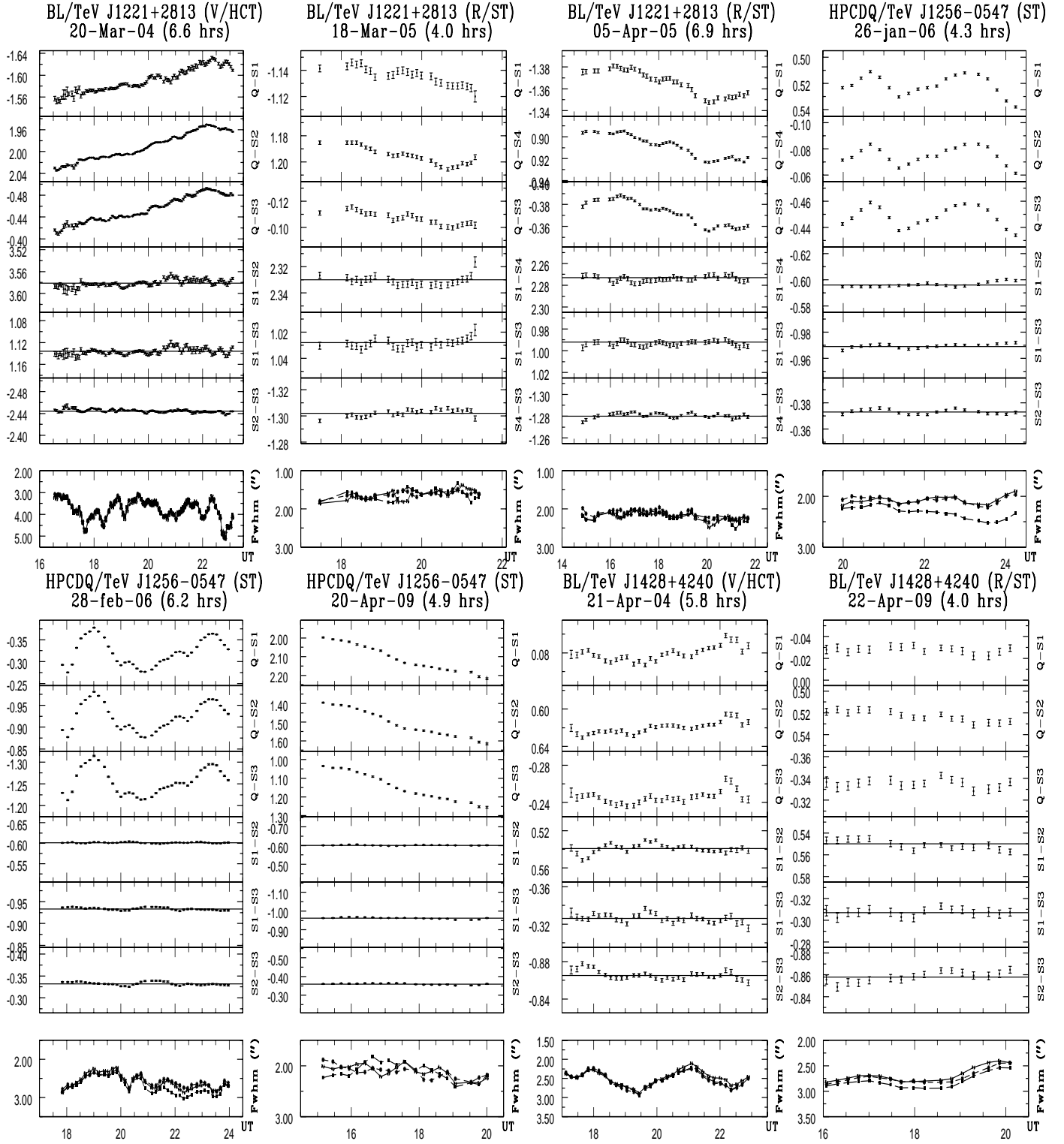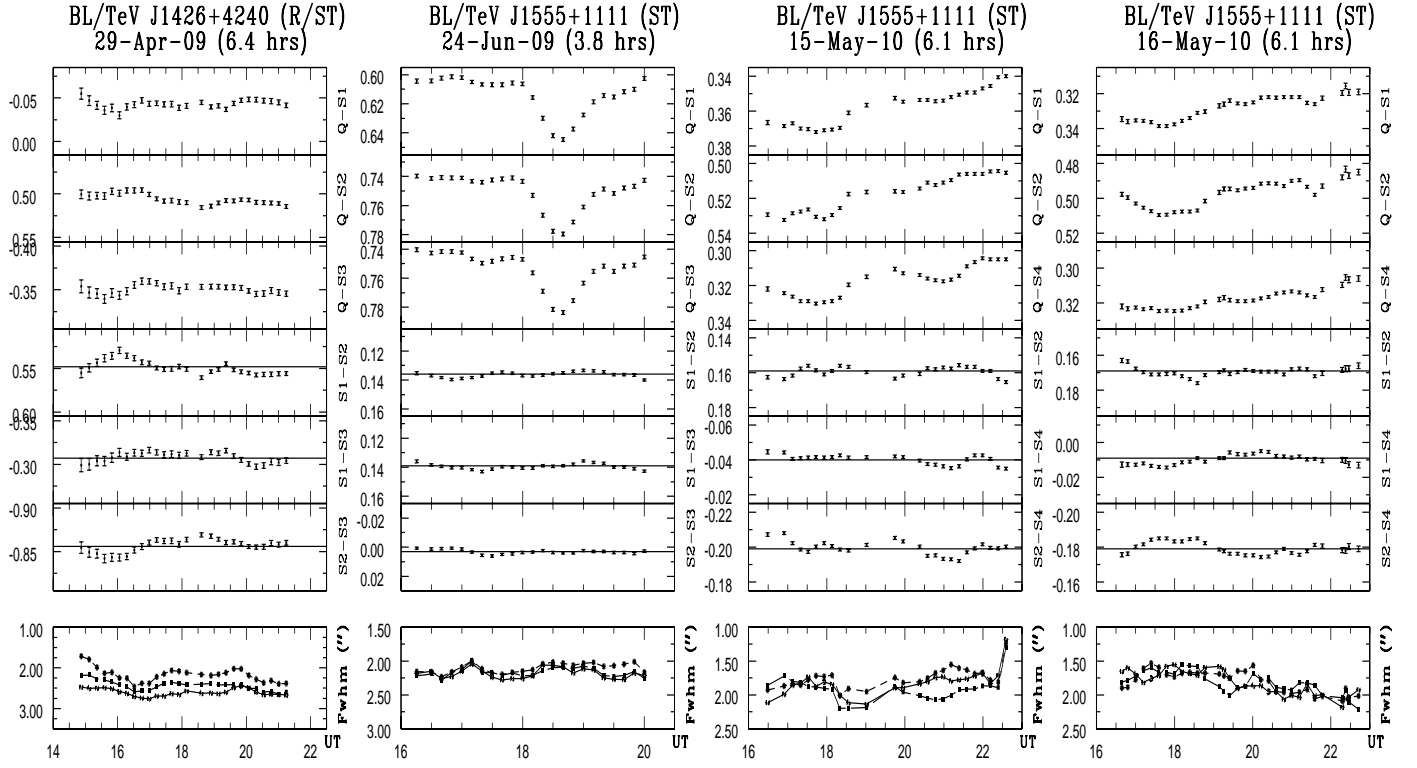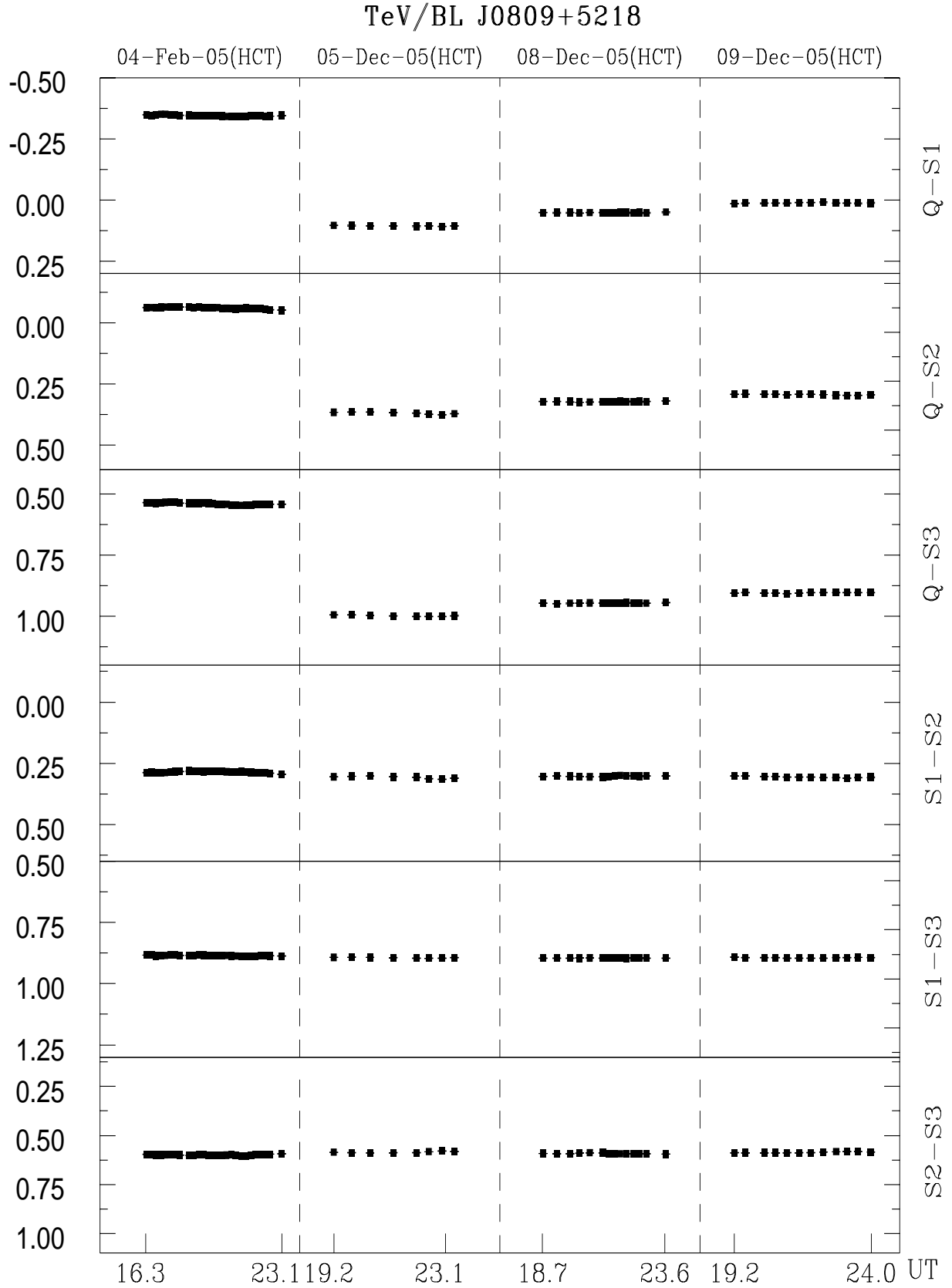
Figure 1. *continued*

Figure 1. *continued*

Figure 1. *continued*

Figure 2. Long-Term Optical Variability (LTOV) DLCs of the TeV blazars in Set 1 (see text).

BL/TeV J1015+4926
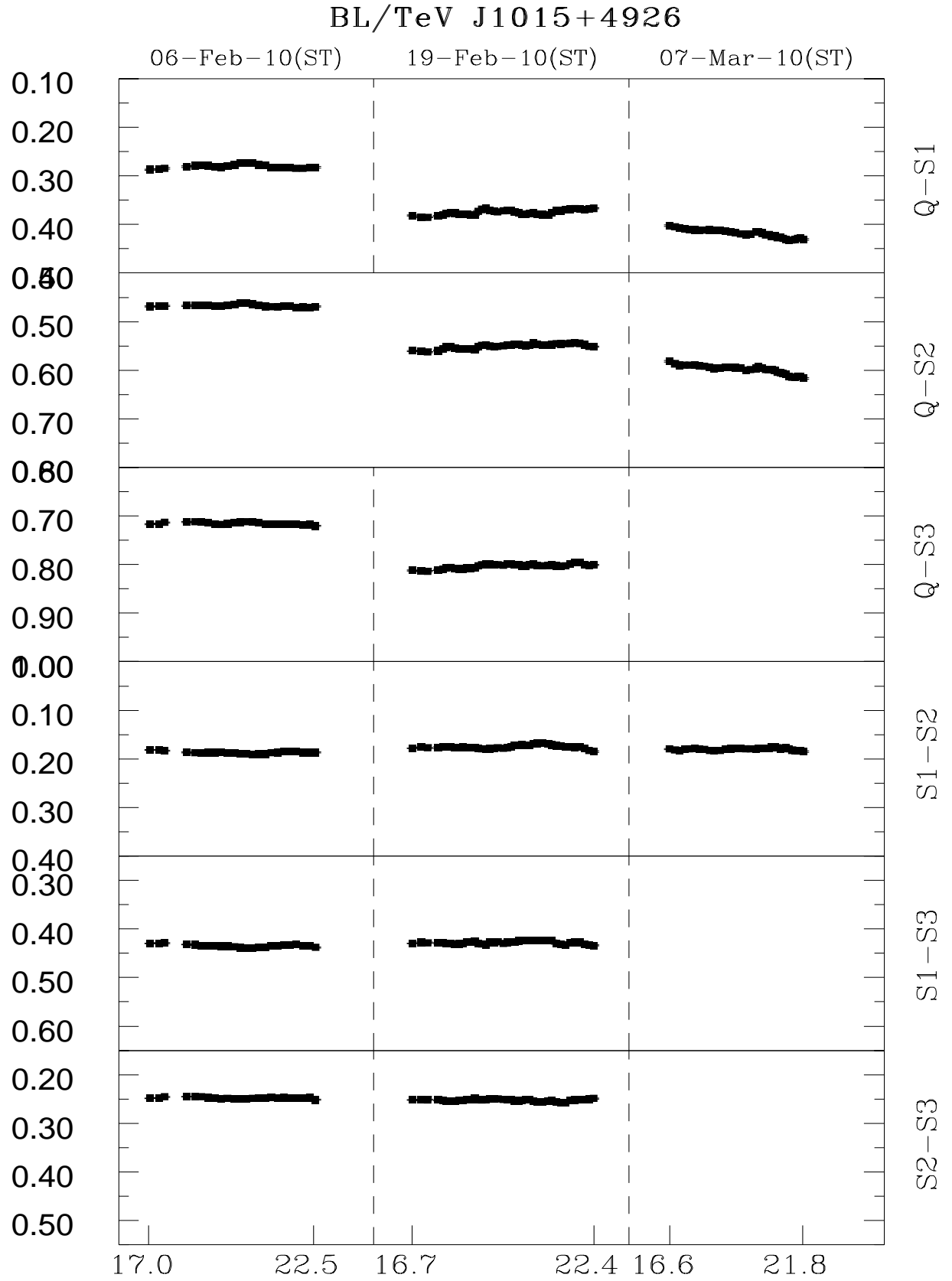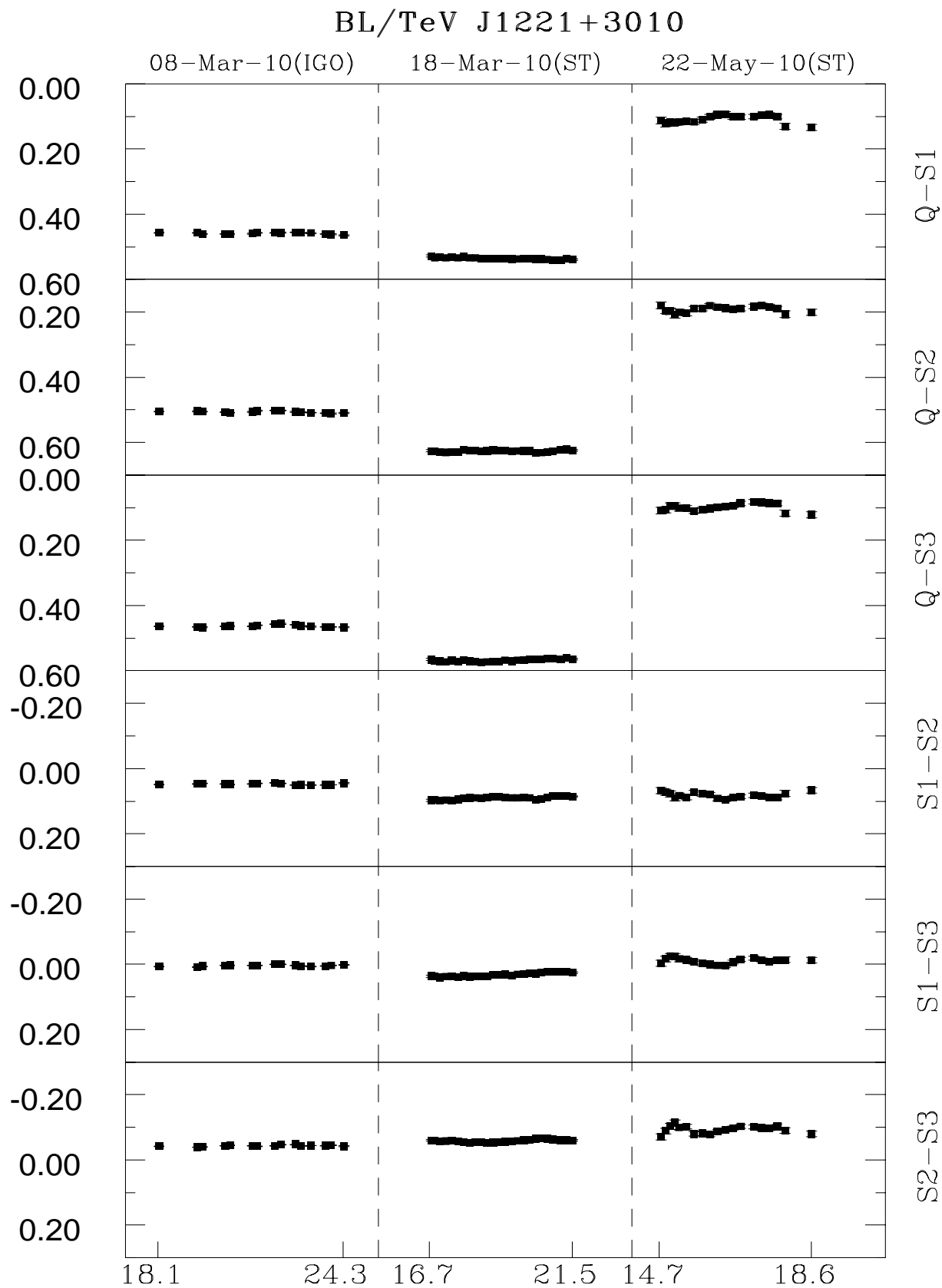
Figure 2. *continued*

Figure 2. *continued*

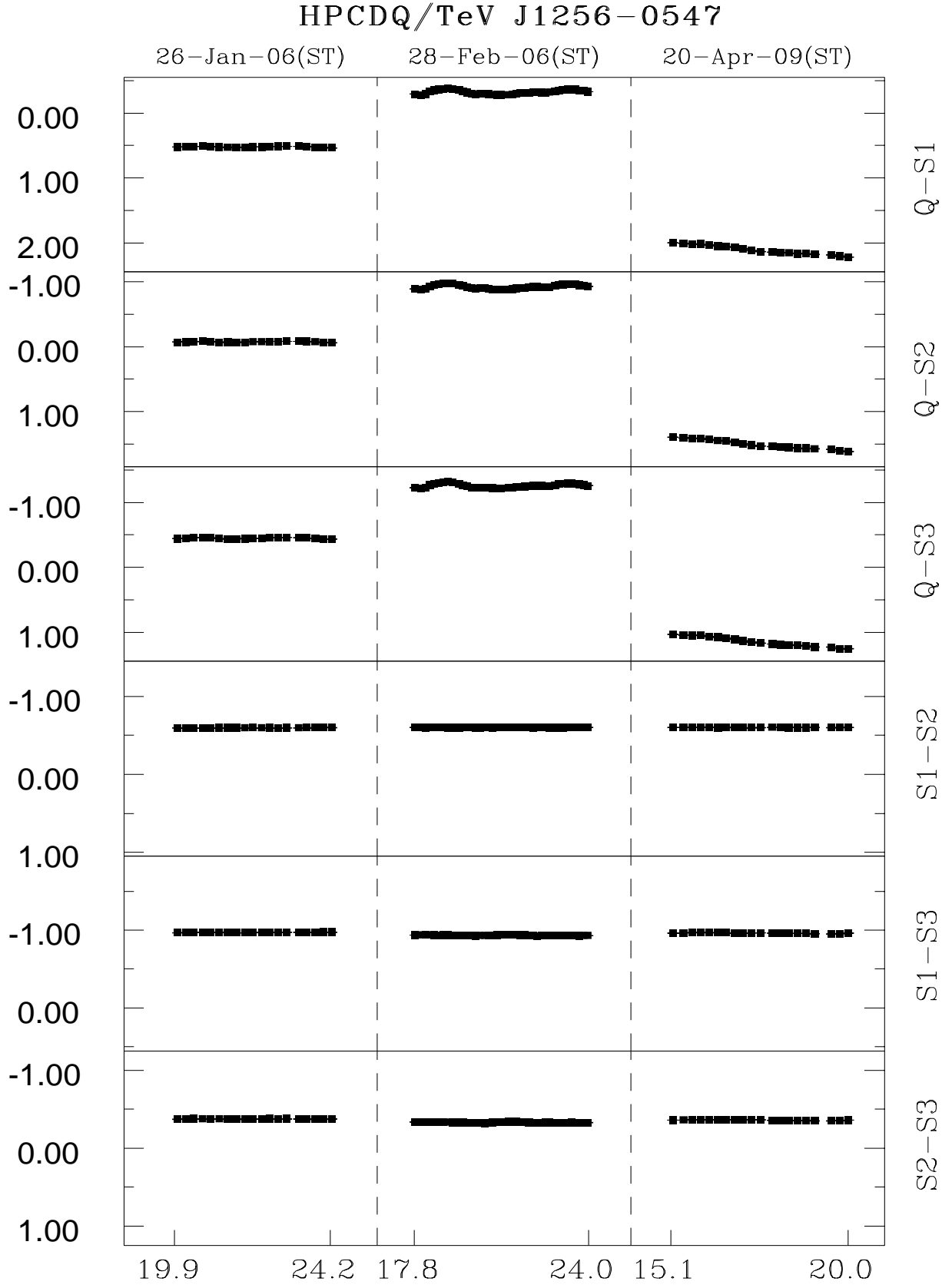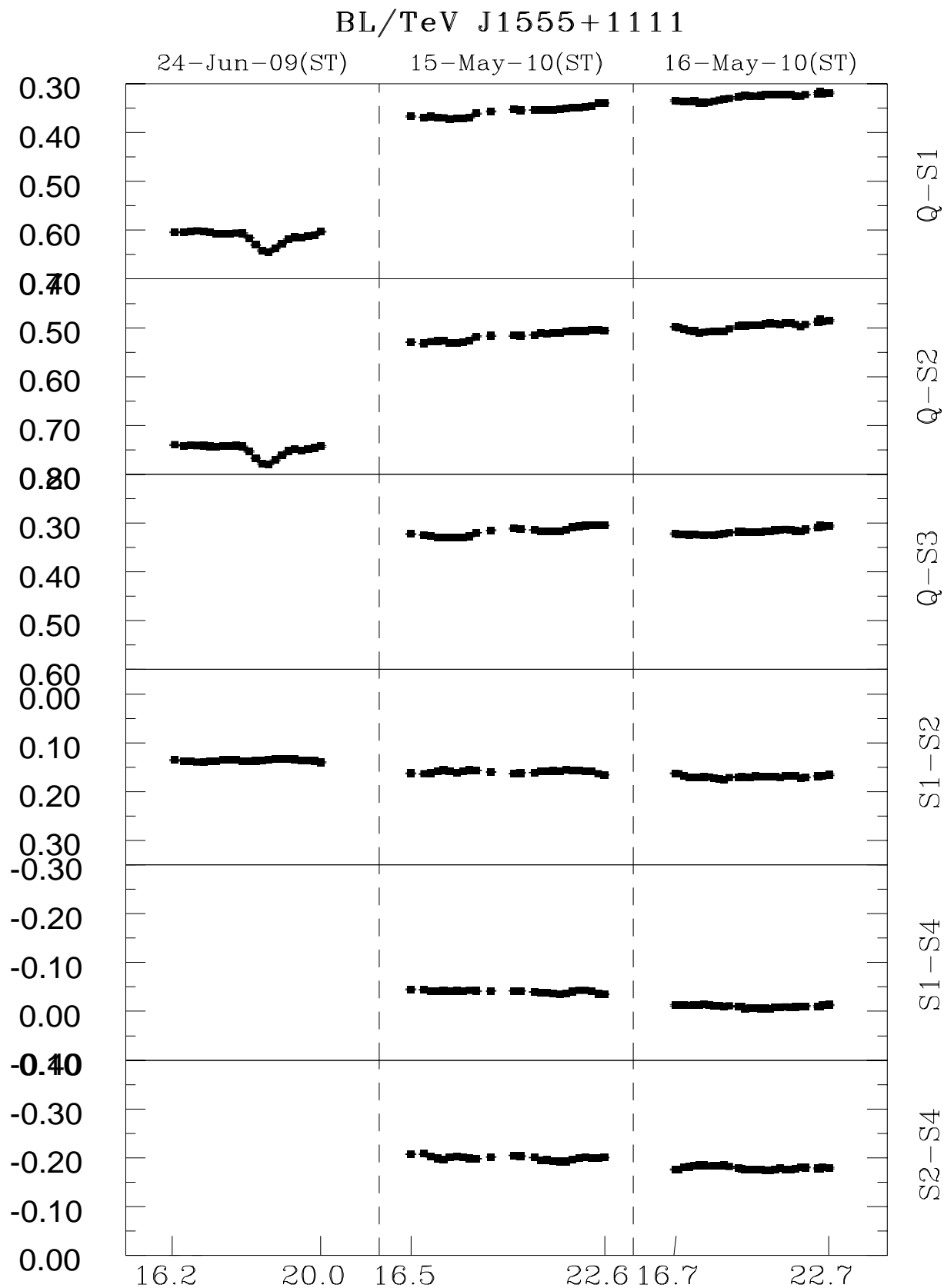# HPCDQ/TeV J1256−0547

Figure 2. *continued*

BL/TeV J1555+1111
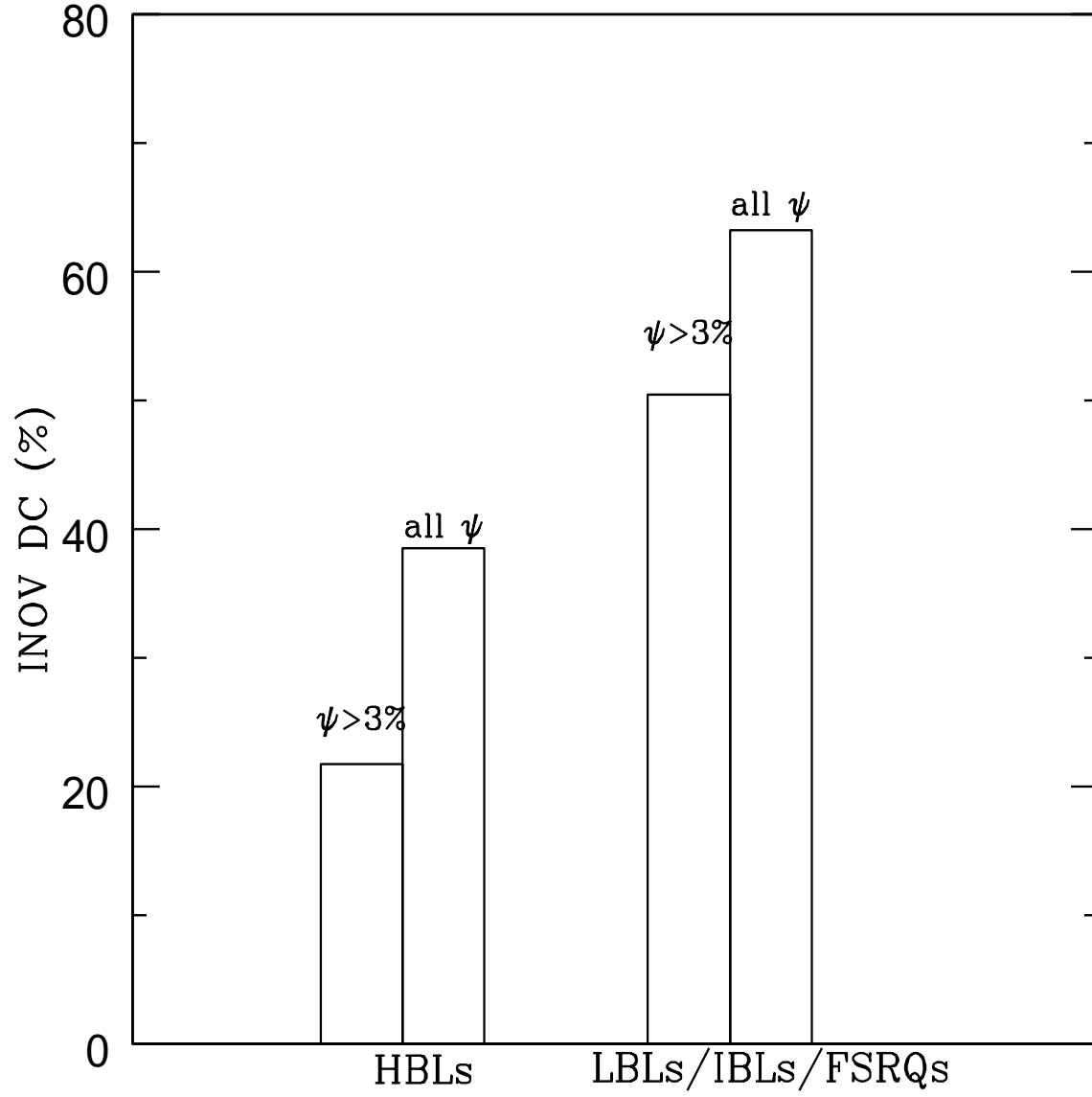

Figure 2. *continued*

Figure 3. Histogram of the INOV duty cycle (present work) derived for the different blazar classes, for two ranges of INOV fractional amplitude ψ.